

# Geomechanics Notes

Robert S. Anderson  
University of Colorado  
November 2018

## Section II - Fluids

### *Table of Contents*

<b>Chapter</b>	<b>Topic</b>	<b>Page</b>
1	Solids and fluids: classification of fluid flow problems	2
2	Continuity and incompressible fluids	9
3	Development of the Navier-Stokes equation	16
4	Non-dimensionalizing the Navier-Stokes equation: $Re$ , and $Fr$ ...	22
5	Hydrostatics, atmospheric pressure profiles, isostasy	25
6	Couette flow, flow between two plates	29
7	Applications of flow between two plates fracture gaps, topographic ooze and salt tectonics	35
8	Isostatic rebound	45
9	Pipe flow: a model of flow through porous media	50
10	Open channel flow	57
11	Glacier flow: An example of nonlinear rheology	61
12	Settling problems: rising bubbles, falling drops, settling grains and sinking crystals	68
13	The speeds of plates in plate tectonics	73
14	Plumes as instabilities: Introducing the Rayleigh number, $Ra$	79
		<b>85 total</b>

## Introduction to fluids

We now turn our attention to fluids, and introduce fluid mechanics. In this introduction I want to accomplish two things. I want to talk about all the fluid problems we might want to tackle in the earth sciences. For now we'll simply classify them. Then I want to introduce a couple terms that will both help us in the development of the principal equation that organized our thoughts about fluid mechanics, and more importantly helps us to get our head around what a fluid is. I want to make sure we all can distinguish between a fluid and a solid. That seems straight forward, but I want to be formal about it.

### *Classifying fluid mechanics problems according to the boundaries*

The simplest cases we will approach are those in which there is indeed a fluid, but it is not moving. We call these statics problems, or **hydrostatics problems**. Examples we will work include such fundamental features as the profiles of pressure within the ocean, crust, and atmosphere. In all other cases we will be dealing with fluid on the move. It can move either because it is being acted upon by gravity, or because it is being pushed by a difference in pressure from one to another point – a pressure gradient. Imagine flow of magma in a slot between two walls – as in a dike or sill. This is an example of “**flow between two plates**”. It is possible that one of the plates or walls bounding the fluid moves relative to the other. This constitutes what is called Couette flow.

If the fluid is bounded not by plates but by the walls of a pipe, we call it **pipe flow**. This problem was worked by two giants in the field of fluid mechanics, Poiseuille and Hagen, so is commonly called *Hagen–Poiseuille* flow. Examples include magma moving up the conduit in the throat of a volcano, or water flow through a circular cave passage. One can also imagine a model of flow through a granular medium, in which the connected pores constitute a network of pipes.

Objects can also be embedded in a flow. The most simple object is a sphere, and the most simple flow is one in which the fluid is still. But unless the sphere has the same density as the fluid, it will move due to gravity, upward or downward depending upon the sign of the density difference, and will experience a resisting force from the fluid. These are **settling problems**: raindrops in air, quartz in water, bubbles in magma. One can ask what the settling speed is – or the terminal velocity. Or we can ask how long it takes or how far it takes for an object to reach its terminal speed.

Fluids on the earth's surface flow downhill, driven by gravity. Most of these flows occur in a channel, and because the channel has no cap on it, we call this flow situation **open channel flow**. Lava flows down a channel, water flows down a channel, glaciers flow down valleys...which serve as their channels.

Another class of flows we will not address here, but that has relevance to earth sciences, is **jets**. Explosive volcanic eruptions of course immediately come to mind.

But the exit of water from a river channel into a still body of water, like the ocean or a lake, also constitutes a type of jet.

In many of these problems our strategy will be to derive the equation representing the profile of flow speed with distance from a boundary, be it a channel bed or a pipe wall. We will then extract formulas for other relevant quantities – like the mean speed, the maximum speed, or the total discharge of the fluid.

### *Flow behavior classification*

In all of the flow cases listed here, there exists a range of flow behavior that depends not on the boundaries, or the boundary conditions, applied to the flow, but to the flow speed in some fashion. The flow, for example, can be very smooth, or it can be very wiggly or swirly. The former we call **laminar**, the latter **turbulent**. In some cases momentum in the flow can only be transmitted downstream, and in others both up and downstream. In this case we talk about **critical** versus **subcritical** flow. Or it might be moving faster than pressure waves can move in the flow. Here we talk about **subsonic** vs. **supersonic** flow. In each case, whether the flow behaves one way or the other depends upon the ratio of two quantities representing the efficiency of certain processes. In the case of turbulence, for example, the behavior depends upon the relative efficiency of transport of momentum by molecular collisions (diffusion) versus advection of momentum by macroscopic swirls or eddies in the flow. We will see that this ratio is a dimensionless quantity that is so important in fluid mechanics that we give it a name, the Reynolds number, denoted  $Re$ . And for each of these transitions in behavior there is such a ratio and associated dimensionless number. These numbers are all named for dead white guys who happened to be important in working on one or another class of fluid mechanics problems. For example, you have no doubt heard of the Mach number,  $Ma$ , which is the ratio of the flow velocity over the speed of sound.

### *Preliminaries: material response to stresses*

Have you ever thought about what a fluid is? And how it differs from a solid? We think of the solid being stiffer than a fluid, right? But I want to get a little more formal than that. They are in fact fundamentally different.

#### **Solids**

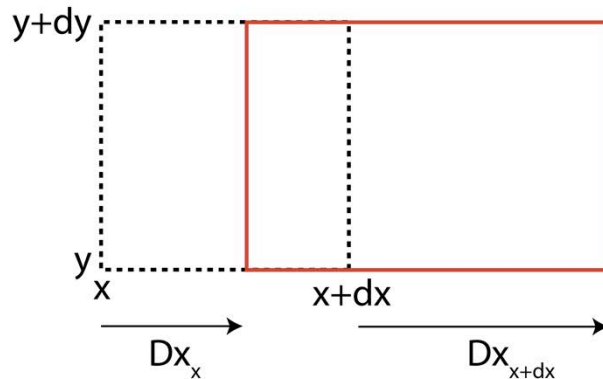
Consider a spring or a slinky. These are appropriate models for a solid in which the molecules are linked by forces that are represented by springs. The spring has an equilibrium length, its length when no force is applied to it. And it stretches or compresses depending upon the applied force. Remember Hooke's law, in which the displacement (how much the spring stretches) is linearly dependent on the force applied:  $F=-kx$ . Here  $k$  is the spring constant. And note that when we remove that force, the spring springs back to its happy position. The displacement is said to be "recoverable". Let us get more precise with our language. Take the original spring of length  $L_o$ . We stretch it so that its length is now  $L_o+dL$ . We define the **strain** of the spring as the change in length divided by the original length:

$$\varepsilon = \frac{\Delta L}{L_o} \quad (1.1)$$

This quantity is therefore dimensionless. A strain of 0.1 means that the item is 10% longer than it used to be. This is called a linear strain (which is all a spring can do). It stretches in the direction of its one-dimensional length.

But in a three-dimensional object, there are other options. Consider for example the cross section of a cube of material depicted in Figure 1. Again, let us stretch the box in the x-direction as in (A). This is a little more general than the spring, since I am allowing both left and right sides of the box to move, or to be displaced. The right hand side of the box has moved more to the right than the left side of the box, resulting in a stretching of the box. It has experienced linear strain just as the spring did. The box changed in length by the *difference* in the displacements of the left and right sides. Said another way, it experienced a *linear strain due to a gradient in the displacements*. In this case the relevant gradient is the gradient in the x displacement with respect to x. Note that if both sides of the box moved exactly the same distance, the box would simply have translated and would not have undergone any strain. In that case the gradient in displacement is zero and so too is the strain.

### A linear strain



### B shear strain

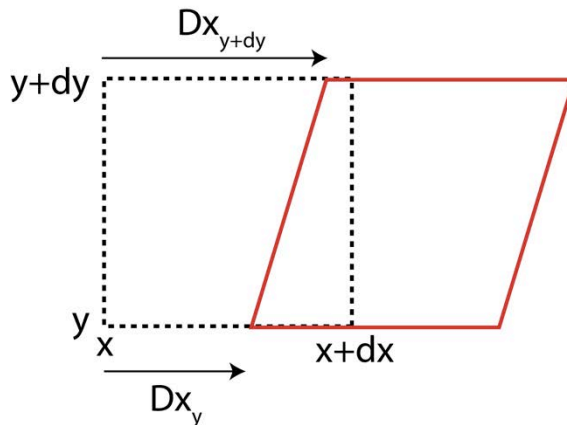


**Figure 1.** Definitions of strain. A) Linear strain results from gradients in displacement in the direction of displacement. B) Shear strain results from gradients in displacement in a direction other than the displacement.

But the box can change shape in another way as well. Consider the diagram (B), in which the top of the box is moved more to the right than the bottom of the box. The shape has changed from a square to a parallelogram. This change in shape is also called a strain, but this time we call it a **shear strain**. How do we measure this? No sides have changed length. But angles have changed. What was originally a right angle between sides is now no longer right. We measure shear strain by the change in angle (which is also dimensionless as radians have no units). In the example shown, the angle may be denoted  $dx/dy$ . This is formally the tangent of the angle, but for small displacements the tangent is the same as the angle (recall the small angle approximation). Note that again we can say that the strain, here a shear strain, resulted from a gradient in the displacements. This time the gradient in the displacement is the gradient in the  $x$  displacement with respect to  $y$ .

So, to summarize, strains in solids result from gradients in the displacements of the material.

As in springs, the strains result from applied forces. But here what matters is not the force applied but the force applied per unit area of the material. And we call this quantity a **stress**. If it is applied normal to a surface of the material we call it (guess what!?) a **normal stress**. If it is applied parallel or tangential to the surface, we call it a **shear stress**. Normal stresses result in linear strain of a solid material. Shear stresses result in shear strains of the material. And if these stresses are removed, the material recovers its original shape. (Unless of course it breaks or fractures, meaning that the strain exceeded a limit of material failure). The material response to a stress is called its **rheology**. For a solid, therefore, the rheology is represented by a plot of strain vs stress, as in Figure 2.

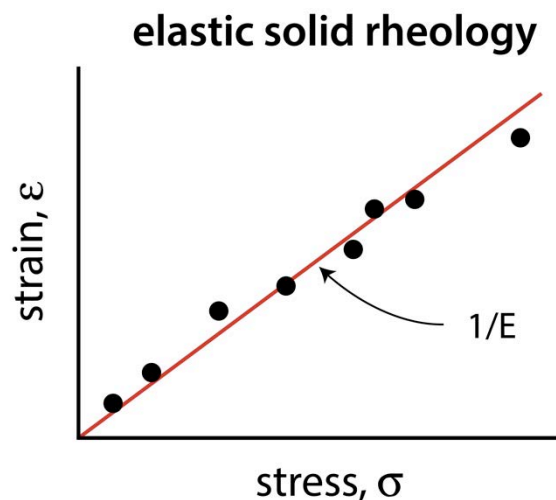


**Figure 2.** Rheology plot for a solid material. Slope of the relationship between strain and stress is the inverse of the Young's modulus,  $E$ .

Strain is commonly denoted  $\varepsilon$ , whereas stresses are commonly denoted  $\sigma$  (for normal stresses) and  $\tau$  (for shear stresses). The mathematical representation of a linear elastic rheology is therefore

$$\varepsilon = \frac{1}{E} \sigma \quad (1.2)$$

Here  $E$  is called Young's modulus. As strain is dimensionless,  $E$  must have the same units as stress, so Pascals (Pa) in the mks or SI system. Such materials are called Hookean in that they obey Hooke's Law, or linear elastic solids.

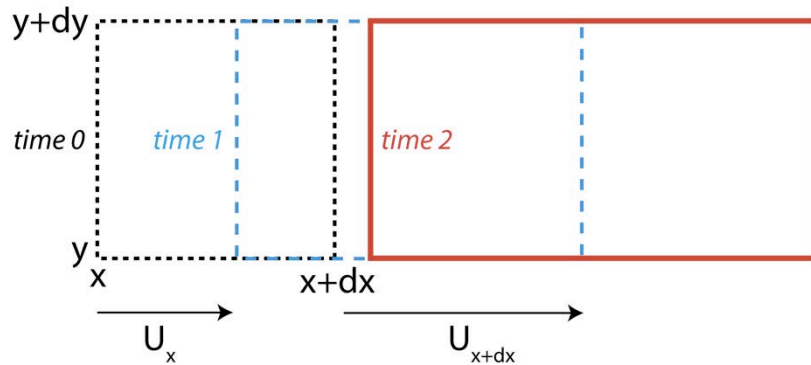
### Fluids

How do fluids differ from solids? First of all the deformation of the fluid is not recovered if we take off the force. Pour honey on a plate. Tip the plate so that it flows (here under the force of gravity). Tip the plate back to flat. It does not reverse its flow to recover its original position on the plate. Its deformation is said to be permanent or non-recoverable.

Not only that, but the strain that is accomplished by applying a stress keeps increasing with time. Back to that honey on a plate: the shear strain that is occurring keeps getting greater the longer the plate is tipped. Put another way, the longer the shear stress due to the component of gravity that is acting parallel to the plate is kept on, the greater the displacement of the top of the fluid relative to where it used to be. The material response to a stress therefore cannot be captured by a relationship of the sort we use to describe a solid. Time seems to matter.

It turns out that if we use velocity instead of displacement, we can develop a description of the fluid's response to stress in a way that is otherwise quite analogous to that of a solid. First, we define the rate of change of strain as how rapidly a parcel of fluid is changing lengths, or changing angles. Its units must be  $1/T$ , as strain is dimensionless. A material strains at a rate that is governed by the gradients in velocity (Figure 3). If one side of the box is moving at a rate that is greater than another side, the box will clearly change shape (stretch or shear). And the rate at which that change in shape occurs depends upon the difference in the speed of the two sides. Such differences in speeds we call gradients in velocity. In Figure 3A we show a situation in which the right hand side of the box is moving at a rate that is greater than the left hand side. Shown at one instant, the box has stretched a certain amount...but shown at a later time, it will have stretched yet more. The rate of strain is equivalent to the gradient in the speed:  $dU/dx$  in this instance. Note the units of a gradient in velocity:  $(L/T)/L = 1/T$ . It has the same units as a strain rate, as it must! And the shear strain rate depicted in Figure 3B, or the rate of change of the angles in the box, is accomplished by a gradient in the  $y$ -direction of the  $x$ -component of velocity,  $U$ , hence  $dU/dy$ .

### A. linear strain rate: $dU/dx$



### B. shear strain rate: $dU/dy$

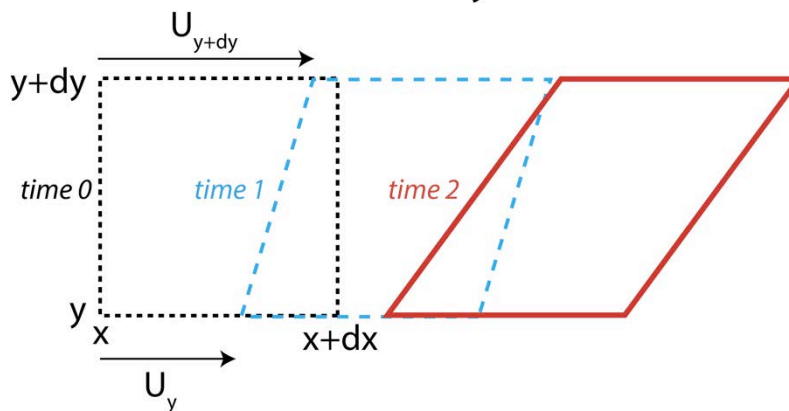


**Figure 3.** Definitions of strain rate. Boxes shown at original shape at time 0, and at two subsequent times. The strain continues to accumulate, while the strain *rate* is steady. A) Linear strain rate results from gradients in velocity in the direction of motion, e.g.,  $dU/dx$ . B) Shear strain rate results from gradients in one component of velocity in some other direction, e.g.,  $dU/dy$  as depicted.

But what is the rheology of a fluid, how do we describe its response to a stress? From experiments, some first described by Newton, we find that for many (but not all) fluids there is a linear relationship between the shear strain rate and the applied stress. In other words,

$$\dot{\epsilon}_{yx} = \frac{dU}{dy} = \frac{1}{\mu} \tau_{yx} \quad (1.3)$$

where the constant  $\mu$  is called the viscosity. Note that the dimensions of viscosity must therefore be the product of stress with time, or Pascal-second (Pa-s) in the mks system. This is plotted in Figure 4. Here I have illustrated with a shear strain in the x-y plane, but this relationship would hold in other dimensions. We will delve more deeply into the notation in the development of the Navier-Stokes equation soon, but for now just know that the two indices on the shear strain rate and the shear stress correspond to the face on which a force is acting and the direction in which it is acting.

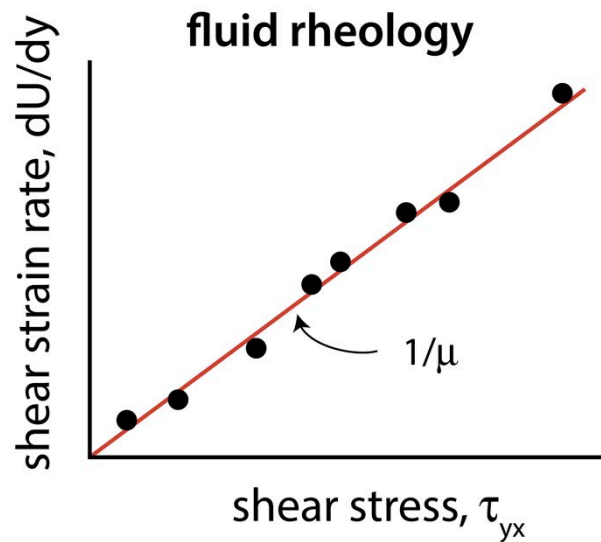


**Figure 4.** Linear viscous rheology. Slope of the relationship between strain rate and stress is the inverse of viscosity,  $\mu$ .

The relationship plotted and expressed mathematically in equation 2 describes a Newtonian fluid, or linear viscous fluid, linear because it is represented by a straight line on a plot of strain rate vs stress.

### Summary

In summary, we have introduced several types of fluid flow situations, both in terms of the boundaries to the flow, and in terms of the flow behavior. In anticipation of the development of the Navier-Stokes equation to come, we have carefully defined terms we will need in that development, in particular stresses, strains and strain rates.

## Continuity: Conservation of Mass



**Figure 1.** Variegated Glacier, Alaska after its 1982-83 surge. The highly crevassed surface is characteristic of a recent surge, as each parcel of ice near the surface has experienced high lateral and longitudinal strain histories.

One of the most general and most powerful statements one can make in the earth sciences is that mass must be conserved. In this section we will formalize this statement to arrive at a compact form that we can then manipulate for special cases. The case on which we will focus is that in which the material is incompressible, as this is indeed true in most geological and certainly most geomorphic problems. As a point of terminology, when you hear someone say “by appeal to continuity”, they typically mean “when mass is conserved”.

Consider a fixed volume with sides  $dx$ ,  $dy$  and  $dz$ . We call this the **control volume** in the problem, and can dictate that it does not change in size. The word statement for conservation of mass in this control volume is simply:

The rate of change of mass within a control volume = the sum of the masses leaving or entering through its edges

Mathematically this looks like:

$$\frac{\partial(\rho dx dy dz)}{\partial t} = \text{inputs} - \text{outputs} \quad (2.4)$$

The left hand side represents the rate of change of mass within the control volume of fixed volume  $dx dy dz$  (Figure 2). Note that we have not allowed any sources or sinks of mass within the volume; it can neither be created nor destroyed.

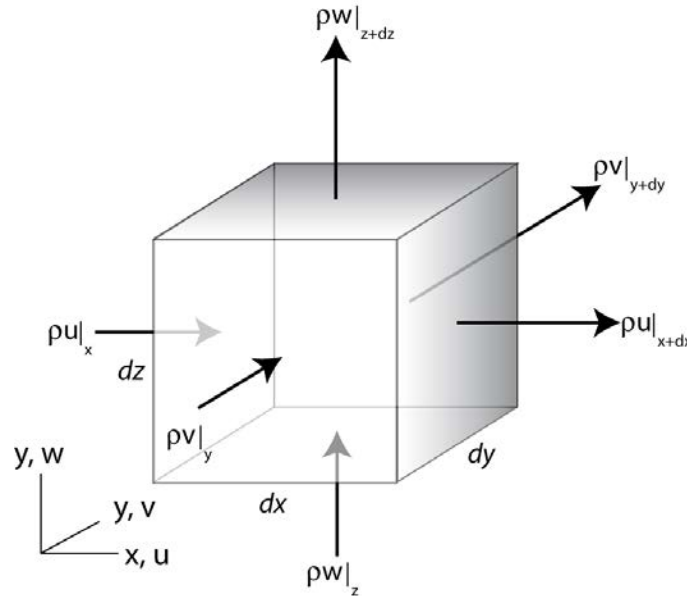


**Figure 2.** Conservation of mass in a control volume  $dx dy dz$ . Rate of change of mass in the volume is governed by rates of arrival and loss of mass across each of the walls. The mass fluxes (arrows) are all positive as depicted. Coordinate system shows  $u$ ,  $v$  and  $w$  components of velocity in the  $x$ ,  $y$  and  $z$  directions, respectively.

We now require expressions for the inputs or outputs of mass through the walls of the control volume. These will be the products of mass fluxes with the areas of the walls. For example, the mass flux across the left wall is  $\rho u$  evaluated at that wall, i.e. at the position  $x$ . Let's make sure we agree that the product  $\rho u$  is a mass flux. The units of this product are  $M/L^3 * L/T = M/L^2 T$ . According to the definition I am using throughout this text, this is indeed a **mass flux**: a mass per unit area per unit time. To determine the total mass transported across the wall per unit time is then the product of this mass flux with the area of the wall. Taking each term in succession, representing total transport of mass across each wall, we now have

$$\frac{\partial(\rho dx dy dz)}{\partial t} = (\rho u)|_x dy dz - (\rho u)|_{x+dx} dy dz + (\rho v)|_y dx dz - (\rho v)|_{y+dy} dx dz + (\rho w)|_z dx dy - (\rho w)|_{z+dz} dx dy \quad (2.5)$$

This is a very general statement for conservation of mass, or **continuity**. We may divide through by the volume of the parcel to simplify this, and collect terms on the right hand side so that they are recognizable as derivatives:

$$\frac{\partial \rho}{\partial t} = - \left[ \frac{(\rho u)|_{x+dx} + (\rho u)|_x}{dx} \right] - \left[ \frac{(\rho v)|_{y+dy} + (\rho v)|_y}{dy} \right] - \left[ \frac{(\rho w)|_{z+dz} + (\rho w)|_z}{dz} \right] \quad (2.6)$$

Acknowledging that as the element shrinks, in the limit as  $dx, dy, dz \rightarrow 0$ , each of the terms in square brackets is a derivative, this simplifies to

$$\frac{\partial \rho}{\partial t} = - \frac{\partial(\rho u)}{\partial x} - \frac{\partial(\rho v)}{\partial y} - \frac{\partial(\rho w)}{\partial z} \quad (2.7)$$

Each of the terms on the right side represents accumulation or loss of mass due to gradients in transport in a particular direction. Make sure you understand why the minus signs are there. Consider the first term as an example. The derivative is positive when more mass leaves across the right hand wall than arrives through the left hand wall. This should reduce the mass in the box, and the negative sign assures that this is the case: positive gradients in mass flux lead to negative rate of change of mass in the box.

So far, we have assumed nothing at all about the substance being conserved. It could for all we know be the mass of ice in a glacier or the mass of fish over a shoal or the mass of peas on your plate. What is the next step? The next step is to recognize that the quantities on the right hand side are products of density and speed, both of which, in general, are variables. We must therefore use the product rule to expand each of these derivatives. While this procedure will double the number of terms on the right, it will allow us to recollect them into two groups with different meanings.

$$\frac{\partial \rho}{\partial t} = -\rho \frac{\partial u}{\partial x} - u \frac{\partial \rho}{\partial x} - \rho \frac{\partial v}{\partial y} - v \frac{\partial \rho}{\partial y} - \rho \frac{\partial w}{\partial z} - w \frac{\partial \rho}{\partial z} \quad (2.8)$$

Moving to the left hand side those terms with density derivatives, and factoring out the density from the remaining terms on the right hand side leaves

$$\frac{\partial \rho}{\partial t} + u \frac{\partial \rho}{\partial x} + v \frac{\partial \rho}{\partial y} + w \frac{\partial \rho}{\partial z} = -\rho \left[ \frac{\partial u}{\partial x} + \frac{\partial v}{\partial y} + \frac{\partial w}{\partial z} \right] \quad (2.9)$$

We can now recognize the left hand side as the total derivative (or substantial derivative, or derivative following the material; see the discussion of the substantial derivative when we first talked about advection). When the derivative of some quantity following the fluid is zero, it means that that quantity is not changing as the material moves. In this case, the quantity is density; in the case in which it does not change while following the parcel, the material is said to be **incompressible**. In other words,

$$\frac{D\rho}{Dt} = 0 \quad (2.10)$$

is shorthand for an incompressible material. Under such conditions, then, the left hand side of equation 6 goes to zero, we can divide by  $(-\rho)$ , and the continuity equation reduces to

$$\frac{\partial u}{\partial x} + \frac{\partial v}{\partial y} + \frac{\partial w}{\partial z} = 0 \quad (2.11)$$

**This is the equation for continuity for an incompressible medium.** The shorthand for this equation, in vector notation, is

$$\nabla \cdot U = 0 \quad (2.12)$$

where both the “del operator” and the velocity  $U$  are vectors. Whether in the component notation or vector notation, this incompressible form of the continuity equation is very commonly the first equation in a paper on fluid mechanics. Because it is so common, it is worth absorbing deeply. Each of the terms in equation 8 is a strain rate. They are equally well called gradients in velocity or strain rates. Their units are  $(L/T)/L$ , or  $T^{-1}$ . If the material is incompressible, then a positive strain rate in one dimension must be compensated by a strain rate in one or the other or both other dimensions. Say there is a positive gradient in speed in the  $x$  direction, meaning that  $\partial u / \partial x > 0$ . This means that the material must be stretching in the  $x$  direction as it moves. If the material is incompressible, it must simultaneously be thinning in at least one of the other dimensions. This thinning, in which particles of material are coming closer together, requires negative velocity gradients.

## The Variegated Glacier surge

We can straight-forwardly apply this concept to explain the pattern of thickening associated with the propagation of a glacier surge down the Variegated Glacier in Alaska in 1982-1983 (Kamb et al., 1985). While most glaciers are well-behaved, and dutifully transport the excess ice arriving in the accumulation zone toward the ablation zone year after year, there to meet its demise by melt, some small fraction of glaciers are not. These ill-behaved glaciers are called surging glaciers. They wait for many years to decades before performing this principal task of a glacier, and then do so in dramatic fashion. Glacier surges require rapid motion of the glacier, which is accomplished by rapid basal motion rather than rapid internal deformation. The surge is typically initiated in the upper reaches of the glacier, and propagates down-valley, bringing with it huge amounts of ice. The pattern of strain experienced by a parcel of ice as it is transported during a surge results in a highly crevassed surface on which one should not even imagine traveling (see Figure 1; map in Figure 3).

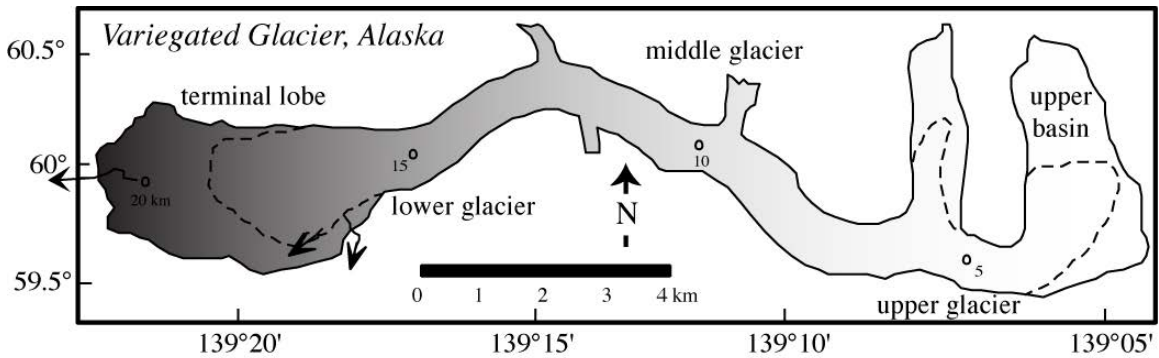


**Figure 3.** Map of the Variegated Glacier, Alaska, showing area of glacier involved in the 1982-83 surge (dashed lines), a few of the km stake locations, and the sites of major outlet streams near the terminus. (after Kamb et al., 2985)

Seen at a fixed location, say through the lens of a fixed camera pointed at the ablation zone, the glacier is at first relatively thin because so little ice has been delivered to the ablation zone for years, and then thickens rapidly as the bulge of the surge arrives. Our task is to understand why this thickening occurs, and at what rate it should occur if we know something about the down-valley pattern of horizontal motion. In other words, for a measured pattern of  $u(x)$ , what is the expected pattern of thickening,  $dH/dt(x)$ ? The pattern of ice speeds, as documented from repeated surveys of stakes on the glacier surface, is shown in Figure 4.

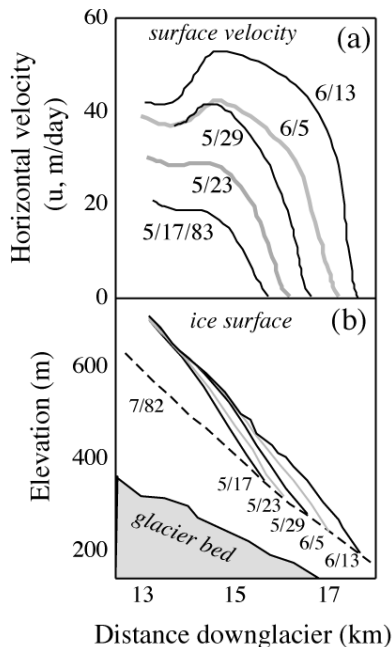


**Figure 4.** a) Ice surface velocity profile,  $u(x)$ , and b) ice surface topography,  $z(x)$ , in a 3-km reach of the lower glacier, during a one-month period of the 1983 surge of the Variegated Glacier (after Kamb, 1985, Figure 4).

The propagation of the surge front into the reach of glacier between km 12 and 18 is clear, as ice speed at a point increases from <1 m/d to > 40 m/d. The spatial pattern of horizontal speed at any time shows a very strong negative gradient of order -20 m/d per km. The pre-surge ice thickness in this reach of the glacier is roughly 150 m (dashed line in (b)). Let's see if we can get in the ballpark with an estimate of the pattern of thickening using our concept of continuity. Our goal is an expression for the expected pattern of vertical velocities at the ice surface, i.e. for  $w(H)$ , where  $H$  is the thickness of the ice. From equation 8, we have

$$\frac{\partial w}{\partial z} = -\frac{\partial v}{\partial y} - \frac{\partial u}{\partial x} \quad (2.13)$$

The rate of change of vertical velocity,  $w$ , with height above the bed,  $z$ , must equal the sum of the gradients in  $x$  and  $y$  speeds. But the glacier is well-confined within its walls, and not much of the crunch associated with the huge gradient in horizontal down-valley speed is taken up by gradients in the lateral direction. So to first order we may ignore  $\partial v/\partial y$ , resulting in this simpler statement:

$$\frac{\partial w}{\partial z} = -\frac{\partial u}{\partial x} \quad (2.14)$$

We need to integrate this equation in the vertical dimension in order to estimate  $w$  at a given height above the bed,  $z$ . In doing so we can make use of another simplification: as the horizontal speeds of a surge are entirely accomplished by basal motion or sliding of the glacier against its bed, they are independent of height above the bed. The glacier is moving like a plug;  $u(z) = U_{slide} = U_{surface}$ . Therefore both  $u$  and  $\partial u/\partial x$  are independent of height above the bed. This means that

$$w(z) = \int_0^z \frac{\partial w}{\partial z} dz = -\int_0^z \frac{\partial u}{\partial x} dz = -\frac{\partial u}{\partial x} \int_0^z dz = -\frac{\partial u}{\partial x} z \quad (2.15)$$

We wish to know the vertical speed at the ice surface, i.e. at  $z=H$ . The final expression for the expected vertical (uplift) speed is

$$w(H) = -\frac{\partial u}{\partial x} H \quad (2.16)$$

The uplift speed or thickening rate of the glacier should be the product of the ice thickness with the local gradient in the horizontal ice speed. The greater the rate at which the column of ice is being squeezed by the horizontal strain rate, and the greater the original height of the column being squeezed, the greater the thickening rate. We can see qualitatively from Figure 4 that this is the case during the Variegated Glacier surge. But let's get quantitative. On May 17th the gradient at km 15, in the middle of the strong speed gradient, is about -20m/d-km (or, stated another way, a horizontal

strain rate of  $0.02 \text{ d}^{-1}$ ), and the pre-surge ice thickness is 175 m. From equation 1.13 we predict a vertical speed of the ice surface of about 3.5 m/d. In the 6 days between May 17<sup>th</sup> and 23<sup>rd</sup>, the ice thickened by about 28 m at km 15. Our calculated total uplift is  $6 \text{ d} \times 3.5 \text{ m/d} = 21 \text{ m}$ . We are indeed in the ballpark.

Now inspect the lead photograph to this section. Seen immediately after the surge of 1982-83, the surface of the Variegated is diced into a city of ziggurats. These intersecting sets of crevasses, some of them many tens of m deep, reflect the strain history to which the surface has been subjected. The first set was longitudinal: it went up and down the glacier. The insertion of these crevasses occurred at a time when the glacier was thickening. It thickened most where the original thickness was greatest: in the centerline. This led to steepening and stretching of the ice surface in the lateral dimension. At the surface, the strain rates must have exceeded the strength of the ice, and it failed in tension to create this crevasse set. At this point the ice is thick, and broken into longitudinal slices. The second set of crevasses occurred after the surge front passed. Note in Figure 3a that the spatial pattern of horizontal speed at any time reaches a peak and then falls off up-glacier. Up-glacier of the peak in surge speed, a positive gradient exists in the glacier speed. For example, on 6/13, the speed increases down-glacier from 41-53 m/d over about 1 km. The  $+0.012 \text{ d}^{-1}$  positive horizontal strain rate would lead to stretching in the down-glacier direction. Indeed, the second set of crevasses is normal to this stretching direction; the ice at the surface again fractured when subjected to such great rates of horizontal strain.

A version of this development was first hung on the web in *The Little Book of Geomorphology* in 2008.

## References

- Kamb, B., C.F. Raymond, W.D. Harrison, H. Englehardt, K.A. Echelmeyer, N.F. Humphrey, M.M. Brugman and W.T. Pfeffer, 1985, Glacier surge mechanism: 1982-83 surge of Variegated Glacier, Alaska. *Science* 227: 469-479.
- Sharp, M., W. Lawson, and R.S. Anderson, 1988, Tectonic processes in a surge-type glacier -- an analogue for the emplacement of thrust sheets by gravity tectonics. *Journal of Structural Geology* 10: 499-515.

## The Navier-Stokes equation

The most famous and most important equation in fluid mechanics is the Navier-Stokes equation. It is application of this equation that leads to solutions for the expected velocity profiles in lava flows, for the discharge of fluid in a pipe, for the flow-field around a settling grain in a fluid. It is also the jumping off point for derivation of velocities in a turbulent fluid.

The Navier-Stokes equation is a highly embellished version of Newton's second law, which states that the rate of change of momentum of an object is the sum of the forces acting on that object. You are no doubt familiar with the form  $F=ma$ , where  $F$  stands for the sum of the forces,  $m$  the mass of the object, and  $a$  its acceleration. Our first task is to rewrite this in the form that better reflects the words:

Rate of change of momentum = sum of forces
--

As usual in these derivations, we expect to arrive at a differential equation reflecting these words.

### *The left hand side*

Recall that the momentum of an object is its mass times its velocity. The velocity is of course a vector, with  $x$ ,  $y$  and  $z$  components. The Navier-Stokes equation is therefore a vector equation. We will develop here one of the three components of this equation, the  $x$ -component. Once this is developed, the other two components can easily be written. Here as usual we will take the object to be our control volume, or box of fluid, with sides  $dx$ ,  $dy$  and  $dz$ . If  $\rho$  is the density of the fluid, the  $x$ -component of the momentum is then  $\rho u dx dy dz$ . We must make a strategic decision about how to proceed. The frame of reference in Newton's case is the object itself: when following along with the object, its acceleration is the sum of the forces acting upon it. This is the Lagrangian frame of reference. If we allow our box of fluid to move about, we are in this frame. If it is held still, tacked down in space, we are in the Eulerian frame of reference. One can get between the two, but one must decide which frame to operate in as we proceed with the derivation. I will choose to work in the Lagrangian frame for now. This means that the rate of change of momentum must be written as if we are following the fluid. The derivative used in this case is the total derivative, or the material derivative, or the substantial derivative, or most informatively, the derivative following the parcel. So the left-hand side becomes

$$\frac{D(\rho u dx dy dz)}{Dt} \tag{3.17}$$

Where  $D/Dt$  is the total derivative operator, and is a shorthand for 4 terms:

$$\frac{D}{Dt} \equiv \frac{\partial}{\partial t} + u \frac{\partial}{\partial x} + v \frac{\partial}{\partial y} + w \frac{\partial}{\partial z} \tag{3.18}$$

The first of these reflects the acceleration at a point, holding  $x$ ,  $y$  and  $z$  constant. The other three terms are called advective terms, and represent the advection of momentum, here the  $x$ -component of momentum. The mathematical signature of an advective term is that it has the form of  $u(dA/dx)$ , where  $u$  is the component of velocity in the  $x$  direction. The quantity  $A$  could be anything: concentration of heat (temperature), concentration of momentum, concentration of fish...

While we can easily factor out the volume of the parcel,  $dxdydz$ , from this expression, we cannot easily separate the density from the velocity. We must chain rule each of the four terms that the total derivative represents. After some rearrangement, this yields

$$dxdydz \left[ \rho \left( \frac{\partial u}{\partial t} + u \frac{\partial u}{\partial x} + v \frac{\partial u}{\partial y} + w \frac{\partial u}{\partial z} \right) + u \left( \frac{\partial \rho}{\partial t} + u \frac{\partial \rho}{\partial x} + v \frac{\partial \rho}{\partial y} + w \frac{\partial \rho}{\partial z} \right) \right] \quad (3.19)$$

or

$$dxdydz \left[ \rho \frac{D(u)}{Dt} + u \frac{D(\rho)}{Dt} \right] \quad (3.20)$$

Note that in the incompressible case, the total derivative of density is zero, and the second term vanishes.

### *The right hand side*

The forces acting on this parcel of fluid come in two flavors: the body force,  $F_b$ , and the surface tractions,  $F_t$ .

$$\sum F = F_b + F_t \quad (3.21)$$

The body force acts on the center of mass of the fluid, while the surface tractions act on the sides of the body. The body force with which we are concerned in geomorphology is that due to gravity: the weight of the parcel. (The other is magnetic force). The component of the fluid weight acting in the  $x$ -direction is simply the mass of the fluid times the component of the acceleration due to gravity in the  $x$ -direction,  $g_x$ , or

$$F_{bx} = \rho dxdydz g_x \quad (3.22)$$

It will be this component of gravity in the down-slope direction that drives flow down an inclined plane.

The surface tractions are harder to deal with. These come about from the action of one element of the fluid on another, pushing or pulling it, or shearing it. The problem is that we have to recognize that these fluid forces act in directions that are both normal to a surface and tangential to it, and they act on all faces of the box. In other words, we

have two directions to keep track of: the face on which the force is acting, and the direction in which it is acting. First, since a stress is a force per unit area, a force must be a stress times an area. We are eventually going to sum up all the forces acting in the x-direction. Each of these forces will consist of product of a stress times the surface area of the face on which the stress is acting. To be organized about this, we will obey the sign convention depicted in Figure 1, in which all of the stresses are depicted as positive. Normal stresses are taken to be positive in tension, in other words when they are directed away from the body. Shear stresses are taken to be positive when they act on the “downstream” face of the box, and are acting in the positive x, y or z direction. For example, the normal force acting on the left face of the box, in the x direction is the normal stress,  $-\tau_{xx}$ , where the minus sign reflects the fact that the stress as shown is acting in the negative x direction, times the area of the side of the box,  $dydz$ .

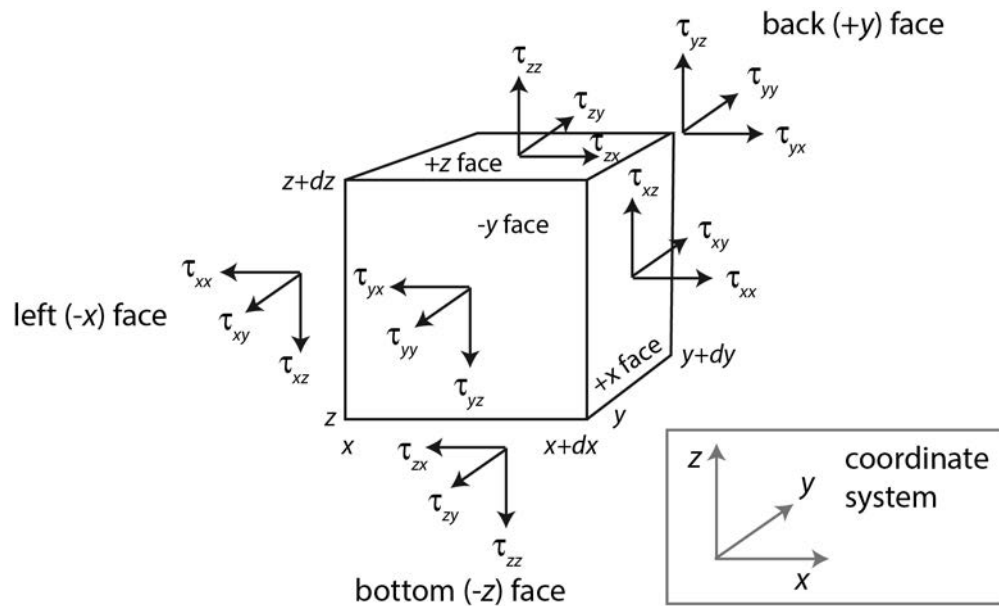


**Figure 1.** Sign convention for stresses on a control volume. (after Anderson and Anderson, 2010, Figure 12.36)

The sum of the surface forces acting in the x-direction is then

$$\begin{aligned}
 F_{ix} = & -\tau_{xx}(x)dydz + \tau_{xx}(x+dx)dydz \\
 & -\tau_{yx}(y)dxdz + \tau_{yx}(y+dy)dxdz \\
 & -\tau_{zx}(z)dxdy + \tau_{zx}(z+dz)dxdy
 \end{aligned}
 \tag{3.23}$$

There is one term for each of the 6 faces of the fluid element. Dividing this expression by the fluid volume  $dx dy dz$ , and recognizing that there are three pairs of terms that reduce to derivatives in the limit as we shrink  $dx$ ,  $dy$  and  $dz$  to zero, allows us to collapse the full force balance equation to:

$$dxdydz \left[ \rho \frac{Du}{Dt} + u \frac{D\rho}{Dt} \right] = dxdydz \left[ \frac{\partial \tau_{xx}}{\partial x} + \frac{\partial \tau_{yx}}{\partial y} + \frac{\partial \tau_{zx}}{\partial z} + \rho g_x \right] \quad (3.24)$$

Dividing through by the mass of the fluid element,  $\rho dxdydz$ , and assuming that the fluid is incompressible ( $D\rho/Dt = 0$ ), yields a general equation for a force balance in the x-direction of an incompressible fluid:

$$\frac{\partial u}{\partial t} + u \frac{\partial u}{\partial x} + v \frac{\partial u}{\partial y} + w \frac{\partial u}{\partial z} = \frac{1}{\rho} \left[ \frac{\partial \tau_{xx}}{\partial x} + \frac{\partial \tau_{yx}}{\partial y} + \frac{\partial \tau_{zx}}{\partial z} \right] + g_x \quad (3.25)$$

We must modify this slightly by recognizing that some stresses result in the distortion of the fluid, a change in its shape, while some result in changes in the size of the fluid element. The mean of the normal stresses acts from all sides and can accomplish a change in volume. We define the *pressure* as

$$P \equiv -\frac{1}{3} (\tau_{xx} + \tau_{yy} + \tau_{zz}) \quad (3.26)$$

where the minus sign represents the tradition that we think about a positive pressure as one that reduces the size of an element, while our convention for normal stresses is that they were defined to be positive in tension. Given this definition of pressure, we can then decompose the stresses into those parts that result in deformation of the fluid element, called the *deviatoric stresses*, from those that can change its volume, the *pressures*:

$$\begin{aligned} \tau_{xx} &= \tau'_{xx} - P \\ \tau_{yy} &= \tau'_{yy} - P \\ \tau_{zz} &= \tau'_{zz} - P \end{aligned} \quad (3.27)$$

where the primes represent the deviatoric stresses. Rewriting each of the stress terms in the force balance equation then results in:

$$\frac{\partial u}{\partial t} + u \frac{\partial u}{\partial x} + v \frac{\partial u}{\partial y} + w \frac{\partial u}{\partial z} = \frac{1}{\rho} \left[ \frac{\partial \tau'_{xx}}{\partial x} + \frac{\partial \tau'_{yx}}{\partial y} + \frac{\partial \tau'_{zx}}{\partial z} \right] + g_x - \frac{1}{\rho} \frac{\partial P}{\partial x} \quad (3.28)$$

This is known as Cauchy's first law, first derived by A. L. Cauchy (1789-1857), a French mathematician (see Middleton and Wilcock, p. 307). Note that we have made no assumptions whatsoever about the nature of the materials involved. This is a very general equation reflecting conservation of momentum in an incompressible fluid. The fluid can be accelerated by either gravity or gradients in either pressure or deviatoric stresses.

But we are not done yet. This equation is said not to be “closed” in the sense that it is not an equation that can be solved for the velocity in the x-direction. The surface tractions, which come in as gradients of stresses, are not represented in terms of the flow speed, or gradients in flow speed. What is needed is a relationship between the stresses and the flow. We have some gut feeling that the flow outside of the box should push or pull or influence in some way the volume of concern. Put another way, the fluid reacts to stresses acting upon it. It does so by deforming at a given rate. This is the essence of a fluid: it responds to stresses by straining at a given rate. There is a unique relationship between stress and strain rate in a given fluid. This relationship is called the constitutive equation, and it describes a rheology (from *rhein*, or flow). It was Newton who first described the most common of these rheologies, which he did by showing experimentally that there exists a linear relation between strain rate and stress. This may be written

$$\frac{\partial u}{\partial z} = \frac{1}{\mu} \tau_{zx} \quad (3.29)$$

This can be solved for the stress, and re-written for each component. Most generally

$$\tau_{ij} = \mu \frac{\partial u_j}{\partial x_i} \quad (3.30)$$

where  $i$  and  $j$  are indices representing  $x$ ,  $y$  or  $z$ . These expressions for stress can be substituted back into the force balance equation, yielding

$$\frac{\partial u}{\partial t} + u \frac{\partial u}{\partial x} + v \frac{\partial u}{\partial y} + w \frac{\partial u}{\partial z} = \frac{1}{\rho} \left[ \frac{\partial(\mu[\partial u / \partial x])}{\partial x} + \frac{\partial(\mu[\partial u / \partial y])}{\partial y} + \frac{\partial(\mu[\partial u / \partial z])}{\partial z} \right] + g_x - \frac{1}{\rho} \frac{\partial P}{\partial x} \quad (3.31)$$

If we treat first a simple system in which the viscosity is both isotropic (all 81 components representing relations between the nine components of the stress and the nine components of strain rate are equal), and does not vary in space, then we are justified in pulling viscosity out of the derivatives, yielding three terms that are dependent upon the curvature of the velocity profile:

$$\frac{\mu}{\rho} \frac{\partial^2 u}{\partial x^2} + \frac{\mu}{\rho} \frac{\partial^2 u}{\partial y^2} + \frac{\mu}{\rho} \frac{\partial^2 u}{\partial z^2} \quad (3.32)$$

The collection of two constants in front of each term arise so commonly in fluid mechanics problems that they have been given their own name, the kinematic viscosity:

$$\nu = \mu / \rho \quad (3.33)$$

which has dimensions of  $L^2/T$ . Our final equation for the conservation of momentum in the x-direction is then

$$\frac{\partial u}{\partial t} + u \frac{\partial u}{\partial x} + v \frac{\partial u}{\partial y} + w \frac{\partial u}{\partial z} = \nu \frac{\partial^2 u}{\partial x^2} + \nu \frac{\partial^2 u}{\partial y^2} + \nu \frac{\partial^2 u}{\partial z^2} + g_x - \frac{1}{\rho} \frac{\partial P}{\partial x} \quad (3.34)$$

This is the x-component of the **Navier-Stokes equation**. The French engineer Claude Navier (1785-1836) and the English mathematician George Stokes (1819-1903) derived this equation in the early 19<sup>th</sup> century, a step beyond Cauchy's first law taken by representing the deviatoric fluid stresses with a viscous rheological law. There are two other equations for the other two components of momentum, y and z, which we will leave to the reader to write. But note before we leave this to explore its application to earth sciences problems that the terms on the right hand side reflect two sources of momentum in a pressure gradient and gravity, and the ability of momentum to be diffused in the fluid in the curvature terms.

The assumptions that we have used to arrive at this from of the equation are:

- The material is incompressible
- The material behaves as a linear viscous fluid
- The viscosity does not vary spatially

**The thermal analogy.** We note that this equation is very similar to that describing the conservation of heat in a conducting medium:

$$\frac{\partial T}{\partial t} + u \frac{\partial T}{\partial x} + v \frac{\partial T}{\partial y} + w \frac{\partial T}{\partial z} = \kappa \frac{\partial^2 T}{\partial x^2} + \kappa \frac{\partial^2 T}{\partial y^2} + \kappa \frac{\partial^2 T}{\partial z^2} + S \quad (3.35)$$

The gravity and pressure gradient terms serve as sources of momentum, just as radiogenic elements serve as the sources of heat,  $S$ , in the general heat equation. The gradients in stresses serve the same purpose as the gradients in heat flow, and are reflected in curvature of velocity on the one hand, and of temperature on the other hand. The analogy is made even tighter by recognizing that the position of the kinematic viscosity in the equation is analogous to the position of the thermal diffusivity. In fact, they have the same units.

Let us classify this Navier-Stokes equation. It is a partial differential equation for  $u$ -velocity (or speed), in that it contains derivatives of both time and all three spatial variables. It is second order, as the highest order of derivative is the second order terms on the right hand side. And it is non-linear, in that the advective terms on the left hand side contain products of the variable  $u$  and its derivatives. It is this latter quality that makes this equation particularly difficult to solve for the most general cases.

Note: This is taken in its entirety from the rivers chapter in Anderson and Anderson (2010).

## Non-dimensionalizing the Navier-Stokes equation

We begin by rewriting the x-component of the Navier-Stokes equation

$$\frac{\partial u}{\partial t} + u \frac{\partial u}{\partial x} + v \frac{\partial u}{\partial y} + w \frac{\partial u}{\partial z} = -\frac{1}{\rho} \frac{\partial P}{\partial x} + \nu \frac{\partial^2 u}{\partial x^2} + \nu \frac{\partial^2 u}{\partial y^2} + \nu \frac{\partial^2 u}{\partial z^2} + g_x \quad (4.1)$$

This is a second order nonlinear partial differential equation (PDE): second order because the highest order derivative is second, partial because it has derivatives in both space and time, and nonlinear because the advective terms in the left hand side contain products of variables and their derivatives. It is therefore messy. As in the thermal problems, we will restrict ourselves to working problems that allow us to make simplifying assumptions. For example, we will work steady problems that will allow us to drop the first term on the left hand side. But just how steady must the system be to justify making this assumption? It is in fact rare that a system is *perfectly* steady, has no change at all in time. We seek a formal way to do this.

It would be immensely helpful to the solution of this complex equation if we could simplify it by being able to ignore one or another term or set of terms. One approach is to determine formally how large each of the terms is in a particular problem. Those that are large relative to others are retained, while those that are small are ignored. This is accomplished by scaling the equation, and converting it to a dimensionless form. Each of the variables can be scaled by a characteristic scale in the particular problem; this is an exercise in normalization. For example, the length scales in a grain settling problem will be the diameter (or the radius) of the particle (the choice is in part dictated by tradition!). The velocity scale in open channel flow might be taken to be either the surface velocity or the mean velocity. This scaling can be achieved by defining

$$T' = t/T, x' = x/L, y' = y/L, z' = z/L, u' = u/U, v' = v/U, w' = w/U$$

These definitions can be used in rewriting the original equation to become

$$\begin{aligned} & \left[ \frac{U}{T} \right] \frac{\partial u'}{\partial t} + \left[ \frac{U^2}{L} \right] u' \frac{\partial u'}{\partial x} + \left[ \frac{U^2}{L} \right] v' \frac{\partial u'}{\partial y} + \left[ \frac{U^2}{L} \right] w' \frac{\partial u'}{\partial z} \\ & = - \left[ \frac{1}{\rho} \frac{P_o}{L} \right] \frac{\partial P'}{\partial x'} + \left[ \frac{\nu U}{L^2} \right] \frac{\partial^2 u'}{\partial x'^2} + \left[ \frac{\nu U}{L^2} \right] \frac{\partial^2 u'}{\partial y'^2} + \left[ \frac{\nu U}{L^2} \right] \frac{\partial^2 u'}{\partial z'^2} + g_x \end{aligned} \quad (4.2)$$

Here we have collected all the scales in the problem into the square brackets. The remaining variables and gradients are not only dimensionless, but should have values that are of the order of 1 to a few, if we have done our scaling correctly (and this is the art of the problem). Importantly, the magnitudes are now all carried by the scales in the brackets. It is by comparing the magnitudes of these collections of constants in brackets that one can assess the relative importance of one or another term in the

equation. There is one more step, which makes this comparison even easier. If we divide all of the terms by the scales in front of, say, the inertial or advective acceleration terms, the resulting equation will be rendered dimensionless. Even more importantly, the dimensionless numbers in front of each term will reflect the importance of that term relative to the inertial terms. Let us do this:

$$\begin{aligned} & \left[ \frac{L}{UT} \right] \frac{\partial u'}{\partial t} + [1]u' \frac{\partial u'}{\partial x} + [1]v' \frac{\partial u'}{\partial y'} + [1]w' \frac{\partial u'}{\partial z'} \\ & = - \left[ \frac{P_o}{\rho U^2} \right] \frac{\partial P'}{\partial x'} + \left[ \frac{\nu}{UL} \right] \frac{\partial^2 u'}{\partial x'^2} + \left[ \frac{\nu}{UL} \right] \frac{\partial^2 u'}{\partial y'^2} + \left[ \frac{\nu}{UL} \right] \frac{\partial^2 u'}{\partial z'^2} + \frac{g_x L}{U^2} \end{aligned} \quad (4.3)$$

Assure yourself that each of the terms in the brackets is dimensionless. These dimensionless numbers, or slight rearrangements of them (their inverse, or one half of them) are the important dimensionless numbers in fluid mechanics. They are

$$\mathbf{Re}, \text{ Reynolds number} = \frac{UL}{\nu}$$

$$\mathbf{Fr}, \text{ Froude number} = \frac{U}{\sqrt{g_x L}} \quad (\text{pronounced Froud; he was Scottish})$$

$$\mathbf{Eu}, \text{ Euler number} = \frac{P_o}{\rho U^2}$$

$$\mathbf{St}, \text{ Strouhal number} = \frac{UT}{L}$$

Given these dimensionless numbers, all named for famous mathematicians and fluid mechanics, we can now re-write the last equation to yield

$$\begin{aligned} & \left[ \frac{1}{St} \right] \frac{\partial u'}{\partial t} + [1]u' \frac{\partial u'}{\partial x} + [1]v' \frac{\partial u'}{\partial y'} + [1]w' \frac{\partial u'}{\partial z'} \\ & = - [Eu] \frac{\partial P'}{\partial x'} + \left[ \frac{1}{Re} \right] \frac{\partial^2 u'}{\partial x'^2} + \left[ \frac{1}{Re} \right] \frac{\partial^2 u'}{\partial y'^2} + \left[ \frac{1}{Re} \right] \frac{\partial^2 u'}{\partial z'^2} + \frac{1}{Fr^2} \end{aligned} \quad (4.4)$$

This is the non-dimensionalized version of the Navier-Stokes equation. It should be clear that the utility of these numbers is that they allow us rapidly to determine the importance of each term relative to the inertial term. Most important for our purposes now is the Reynolds number. Note that if the **Re** is small, then the magnitude of the viscous terms become large compared to the inertial terms. The latter can then safely be ignored. As these inertial terms are the nonlinear ones, this is tremendously useful. The **Re** is small if the product of the length and velocity scales is small compared to the kinematic viscosity. This number was named for Osborne Reynolds (1842-1912), a civil and mechanical engineering professor at Owens College, Manchester, working in the late 19<sup>th</sup> century on the onset of turbulence in flow through tubes, although George Stokes (1919-1903) had pointed out the importance of this collection of constants in

controlling the flow field for particular geometries 40 years earlier (e.g., what we now call Stokes law for the drag force on a sphere; see Batchelor, p.214). Reynolds published a pair of papers that have become pillars in turbulence research (Jackson and Launder, 2007). In the first he reported his experiments on the “tendency of water to eddy” and the control of this tendency by a ratio of scales that now carries his name (Reynolds, 1883). In the second he provides a theoretical approach to averaging of the Navier-Stokes equations (to yield what are now known as the Reynolds equations) as a means of exploring the switching of flows into and out of turbulence (Reynolds, 1895).

## References

- Anderson, R.S. and S.P. Anderson, 2010, *Geomorphology: The Mechanics and Chemistry of Landscapes* (Cambridge University Press) textbook, 640 pp., published June 2010.
- Batchelor, G.K., 1970, *An Introduction to Fluid Dynamics*, Cambridge: Cambridge University Press.
- Jackson, D. and Launder, B., 2007, Osborne Reynolds and the publication of his papers on turbulent flow, *Annual Review of Fluid Mechanics* 39: 19–35.
- Reynolds O., 1883, An experimental investigation of the circumstances which determine whether the motion of water in parallel channels shall be direct or sinuous and of the law of resistance in parallel channels, *Philosophical Transactions of the Royal Society* 174: 935–982.
- Reynolds O., 1895, On the dynamical theory of incompressible viscous fluids and the determination of the criterion, *Philosophical Transactions of the Royal Society* 186:123–164.

## Hydrostatics: Pressure profiles in the ocean and atmosphere

The Navier-Stokes equation is useful even in the simplest of situations. Here we start with what are called statics problems, in which the fluid is in fact stationary. We ask what are the expected profiles of pressure within the ocean and the atmosphere.

We first write the Navier-Stokes equation, our general equation for fluid flow problems. But this time we utilize the z-component of the equation:

$$\frac{\partial w}{\partial t} + u \frac{\partial w}{\partial x} + v \frac{\partial w}{\partial y} + w \frac{\partial w}{\partial z} = -\frac{1}{\rho} \frac{dP}{dz} + \nu \frac{\partial^2 w}{\partial x^2} + \nu \frac{\partial^2 w}{\partial y^2} + \nu \frac{\partial^2 w}{\partial z^2} + g \quad (5.1)$$

Here since we have oriented our z-coordinate vertically, the component of the gravity in this direction is simply  $g$ ; in other words,  $g_z = g$ .

For the problem at hand, we may make the following assumptions in order to simply this equation. First, assume that the problem is steady. That takes care of the first term, as all time derivatives may be taken to vanish in steady problems. In fact, the name “statics” signifies that we are doing even more than this. Not only is the problem steady, but there is no flow in any direction! This means that  $w=0$  everywhere, and the N-S equation reduces to

$$0 = -\frac{1}{\rho} \frac{dP}{dz} + g \quad (5.2)$$

### Pressures in the ocean

Let us first work the problems of the pressure profile in the ocean. For this problems we align our z-axis vertically, with  $z=0$  at the ocean surface, increasing downward, in the direction of  $g$ . Rearranging equation 1, this becomes simply

$$P = \int_0^z \rho_{sw} g dz \quad (5.3)$$

where the subscript on the density denotes seawater. In this case, let us assume that the density of the ocean is uniform with depth. We may then bring both the density and gravity out of the integral, leaving us to integrate  $dz$ :

$$P = \rho_{sw} g \int_0^z dz = \rho_{sw} g z + c \quad (5.4)$$

It remains to evaluate the constant of integration,  $c$ . For this we use a boundary condition. At the top of the ocean, the pressure is simply atmospheric pressure,  $P_{atm}$ . Therefore, we are left with the following pressure profile in the ocean:

$$P = P_{atm} + \rho_{sw}gz \quad (5.5)$$

The pressure linearly increases with depth. Using proper values of the density,  $\rho_{sw}=1030 \text{ kg/m}^3$ , and setting  $P_{atm} = 10^5 \text{ Pa}$ , we can calculate the depth at which the pressure is double that at the surface.  $z=P_{atm}/\rho_{sw}g=9.9 \text{ m}$ . At roughly 10 m depth in the ocean, the additional pressure is equivalent to one atmosphere.

The pressure profile in the earth's crust is identical, except that the relevant density in equation 5 is that of crustal rock:  $3000 \text{ kg/m}^3$  in basalt, and  $2650 \text{ kg/m}^3$  in granite. Performing the same calculation to find what column of rock is equivalent to the column of atmosphere results in about 3 m. Three meters of rock, or about the height of a typical room, generates the same pressure as the entire atmosphere.

### *Pressure profile in the atmosphere*

It would seem that all we have to do to calculate the pressure profile in the atmosphere is turn our z-coordinate around so that it increases upward. We will do that, but a problem arises in that the density of the atmosphere is not uniform with height. In fact we know this at some level because it smoothly vanishes as one approaches outer space. And we know that at high elevations it gets harder to breathe – meaning to get enough oxygen to operate our muscles.

Let's start by turning around our coordinate. Our z coordinate increases upward. And now  $g_z = -g$ . What is left of the Navier-Stokes equation becomes

$$0 = -\frac{1}{\rho} \frac{dP}{dz} - g \quad (5.6)$$

or

$$\frac{dP}{dz} = -\rho g \quad (5.7)$$

It is time to get real about our atmospheric density. The atmosphere is a gas, and we expect that its density will depend upon the pressure. The atmosphere obeys the ideal gas law:

$$PV = nRT \quad (5.8)$$

where  $P$  is pressure,  $V$  is volume,  $n$  the number of moles,  $R$  the universal gas constant, and  $T$  the temperature in Kelvins. We seek somewhere in all this an expression for the density. Recalling that the molecular weight of a gas,  $m_g$ , is the mass of the gas per mole, the density of the gas can be written

$$\rho = \frac{m_g n}{V} \quad (5.9)$$

But we know from the universal gas law that  $n/V=P/RT$ . Substituting for this ratio in equation 9 gives us our relation between density and pressure:

$$\rho = \frac{m_g P}{RT} \quad (5.10)$$

Inserting this relationship into equation 7 yields

$$\frac{dP}{dz} = - \left[ \frac{m_g g}{RT} \right] P \quad (5.11)$$

One can see from inspection of this ordinary differential equation that i) it looks like a radioactive decay equation, and ii) the term in the brackets must have units of an inverse length. Acknowledging this, let us define a length scale by flipping this expression in brackets upside down:

$$h_* = \frac{RT}{m_g g} \quad (5.12)$$

We may now proceed to solve the ODE by separating variables. The first step gives us

$$\frac{dP}{P} = - \frac{dz}{h_*} \quad (5.13)$$

We can integrate both sides to obtain

$$\ln(P) = - \frac{z}{h_*} + c \quad (5.14)$$

We employ a boundary condition to solve for the constant of integration,  $c$ . In this case we use the fact that we can measure the pressure at the base of the atmosphere, say at sealevel. Hence we use  $P=P_{atm}$  at  $z=0$ .

$$c = \ln(P_{atm}) \quad (5.15)$$

Applying this to equation 14 and integrating with respect to  $z$  yields

$$P = P_{atm} e^{-z/h_*} \quad (5.16)$$

Atmospheric pressure ought to decline exponentially with height above sealevel, with a characteristic height  $h^*$ . But what is that characteristic height? Let us evaluate equation 12. The universal gas constant is  $8.314 \text{ J}/(\text{mol}\cdot\text{K})$ . The atmospheric temperature is  $-30^\circ\text{C}$  ( $=243\text{K}$ ; remember that from the one-layer calculation we made earlier?). The acceleration due to gravity  $g = 9.81 \text{ m/s}^2$ . But what is the molecular weight of the atmosphere? We require two things: knowledge of the composition of the atmosphere, and the periodic table. The atmosphere is 78%  $\text{N}_2$  (molecular weight  $2 \times 14 = 28 \text{ g/mole}$ ), 21%  $\text{O}_2$  (molecular weight  $2 \times 16 = 32 \text{ g/mole}$ ) and 1% Ar (molecular weight  $40 \text{ g/mole}$ ). Weighting these gases appropriately, we find that the molecular weight of air is  $28.96 \text{ g/mole}$ , or  $29 \times 10^{-3} \text{ kg/mole}$ . Evaluating the height scale we find that height scale of the atmosphere is  $h^* = 7096 \text{ m}$  or about  $7.1 \text{ km}$ .

Now we can calculate the atmospheric pressure on the top of Everest. This tallest peak on the planet is  $8848 \text{ m}$ , at last measurement. The atmospheric pressure at the summit is therefore  $e^{-8.5/7.1}$  or  $0.29$ . Atmospheric pressure there is only 29% of the atmospheric pressure at sealevel.

The observant reader will have noticed that I have not taken into account the fact that the temperature of the atmosphere in fact declines with height. The profile we have therefore calculated is only approximately correct. It nonetheless captures the essence of the pattern.

## Couette flow and flow between two plates

Let us now consider a situation in which flow occurs between two parallel flat impermeable plates, oriented horizontally. This type of flow in a gap between two surfaces is named for Maurice Marie Alfred Couette, a French physicist who lived from 1858-1943. He was famous for his work on the “friction of fluids” and was responsible for designing the cylindrical viscometer.

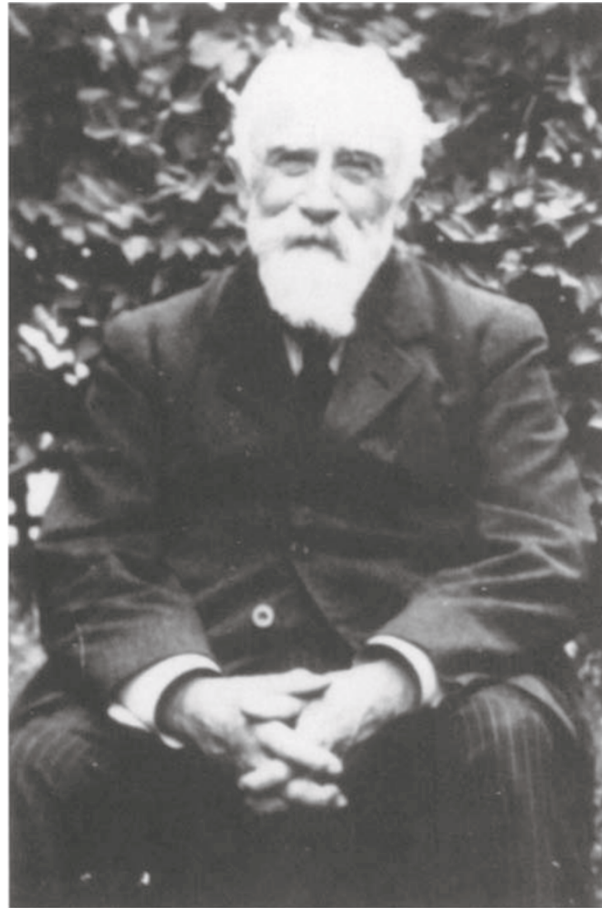


Figure 1. Maurice Marie Alfred Couette (1858-1943). (Piau et al., 1994, Figure 1)

### *Simplifying the Navier-Stokes equation for the problem at hand*

Consider the flow between two flat plates to be uniform, steady, and incompressible (Figure 2). This is plane Couette flow. The flow may be driven by either or both of two actions: 1) a pressure gradient in the  $x$  (horizontal) direction, or movement of one plate relative to the other. For generality, then, we will retain the pressure gradient term in the Navier-Stokes equation.

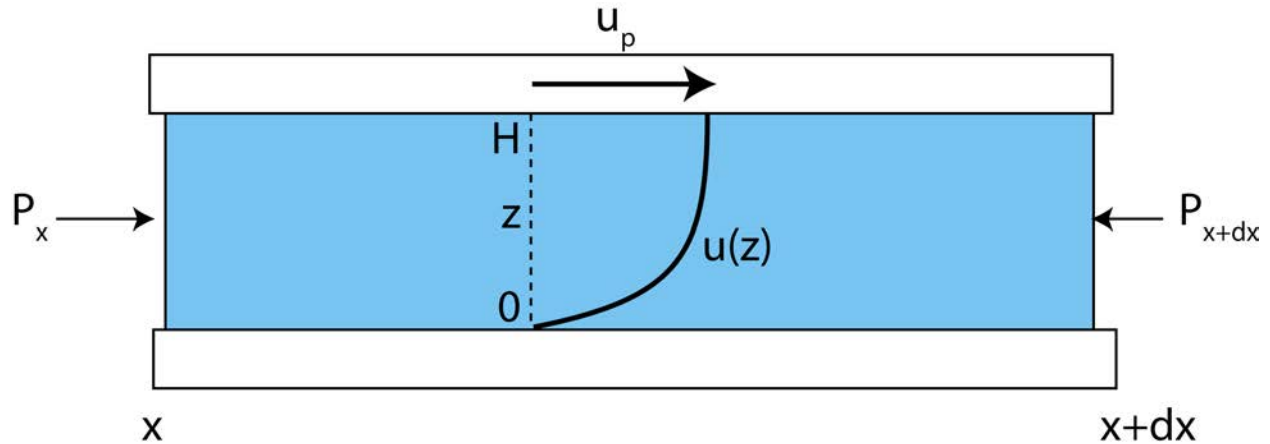


Figure 2. Sketch of flow between two horizontal plates.

Our first task is to reduce the  $x$ -component of the Navier-Stokes equation (1) to retain only the important terms for this particular situation.

$$\frac{\partial u}{\partial t} + u \frac{\partial u}{\partial x} + v \frac{\partial u}{\partial y} + w \frac{\partial u}{\partial z} = -\frac{1}{\rho} \frac{dP}{dx} + \nu \frac{\partial^2 u}{\partial x^2} + \nu \frac{\partial^2 u}{\partial y^2} + \nu \frac{\partial^2 u}{\partial z^2} + g_x \quad (6.17)$$

The first term on the left hand side (lhs) may be safely ignored as the time rate of change is zero, and hence all time derivatives are zero. The flow is being driven only in the  $x$ -direction and is horizontally uniform. Hence all derivatives with respect to  $y$  and to  $x$  are zero. The flow looks the same in any  $x$ - $z$  plane, and does not vary along the  $x$ -direction. This allows the second and third terms on the lhs to vanish.

But what about the last term on the left? As the flow will certainly vary in the  $z$ -direction, the  $du/dz$  will not vanish. What about the  $w$ ? We employ several attributes of the flow to argue that  $w$  is in fact zero everywhere in the flow. First, from the continuity equation, we know that if the flow is incompressible, then  $\frac{\partial u}{\partial x} + \frac{\partial v}{\partial y} + \frac{\partial w}{\partial z} = 0$ . That the flow is

horizontally uniform requires that the first two terms are zero, hence this boils down to the statement that  $\frac{\partial w}{\partial z} = 0$ . And we can integrate this simple equation to obtain  $w =$

constant. But what is the constant? If we know the vertical flow speed anywhere, it is that speed everywhere. Here we appeal to the impermeability of the plates, which demands that no flow cross the plate boundaries, and therefore that  $w = 0$  at the walls. And since  $w$  is a constant with respect to  $z$ , and  $w = 0$  at a wall,  $w = 0$  everywhere. This allows us to neglect the last term on the left hand side.

On the right side, that the plates are horizontal means that there is no body force pushing the flow in the  $x$ -direction, and the last term may be neglected. We must retain the pressure gradient term as it is pushing or pulling the flow (so despite the fact that we have argued that there are no gradients in the flow, the situation still demands a

gradient in the pressure in the x-direction). The last three terms are the viscous terms, the second derivatives of horizontal velocity in the x, y and z directions. That the flow is horizontally uniform allows us to neglect not only first derivatives in x and y, but second derivatives as well. This leaves us with only two terms, and moving the term with  $u$  to the left side yields:

$$v \frac{d^2 u}{dz^2} = \frac{1}{\rho} \frac{dP}{dx} \quad (6.18)$$

This is an ordinary, linear 2<sup>nd</sup> order ordinary differential equation. The left hand side captures the effect of diffusion of momentum by viscosity, whereas the right hand side represents a source of momentum. Using the definition of the kinematic viscosity, it may be rewritten

$$\frac{d^2 u}{dz^2} = \frac{1}{\mu} \frac{dP}{dx} \quad (6.19)$$

### **Solving for the flow profile**

Ok, now we have come to the starting line. We have an equation with the second derivative of the quantity for which we wish to solve, here  $u$ . As is often the case, we now must integrate this equation twice, and apply boundary conditions to evaluate the resulting constants of integration. The first integration yields

$$\frac{du}{dz} = \frac{1}{\mu} \frac{dP}{dx} z + c_1 \quad (6.20)$$

Solving for the constant of integration,  $c_1$ , at this point would require knowing what the gradient in velocity is at some point. Instead, let us proceed, and retain the constant in the second integration:

$$u = \frac{1}{\mu} \frac{dP}{dx} \frac{z^2}{2} + c_1 z + c_2 \quad (6.21)$$

We now have two constants of integration. Since we know that the flow must come to rest ( $u=0$ ) at each of the two walls, we may use “no slip” conditions as our boundary conditions. Let us first use the fact that  $u=0$  at  $z=0$  (the bottom wall). Plugging these statements into equation 5 shows that this requires that  $c_2 = 0$ . That was easy. Now employing  $u=U_0$  at  $z=h$ , the top wall, requires that

$$U_0 = \frac{1}{\mu} \frac{dP}{dx} \frac{h^2}{2} + c_1 h \quad (6.22)$$

which we may solve for  $c_1$ :

$$c_1 = \frac{U_0}{h} - \frac{1}{\mu} \frac{dP}{dx} \frac{h}{2} \quad (6.23)$$

Inserting these values for the constants back into equation 5 yields our general formula for the vertical structure of the horizontal flow field in the channel between the two plates:

$$u = U_0 \frac{z}{h} - \frac{1}{2\mu} \frac{dP}{dx} [hz - z^2] \quad (6.24)$$

In Figure 3 I show this solution for several choices of the speed of the top plate. One can see the solution segue between a parabola for the stationary plate case, toward a linear profile for the no pressure gradient case. In Figure 3, the pressure gradient is the same in all cases.

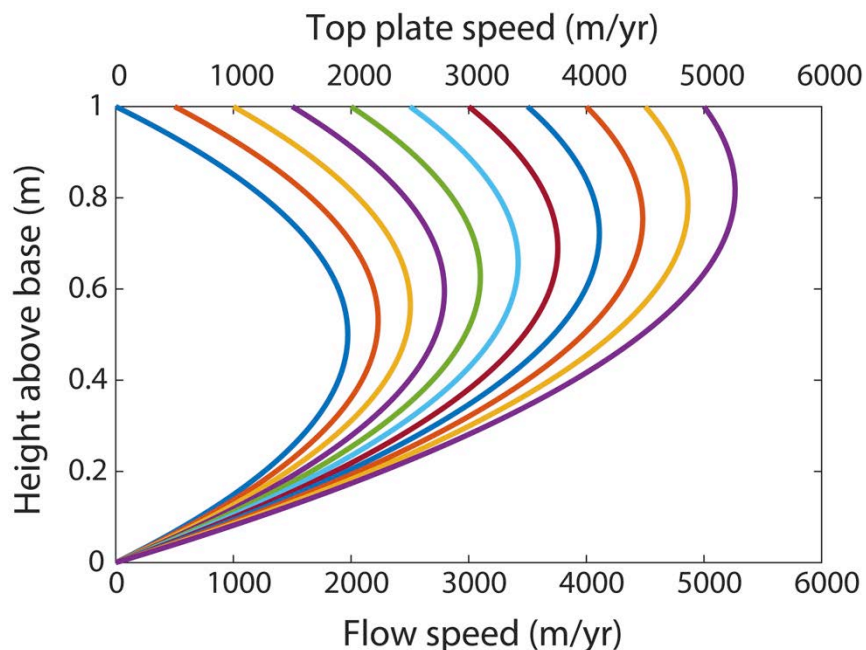


**Figure 3.** Flow between two plates. Basaltic magma with viscosity 500 Pa-s in horizontal 1-m thick channel. Favorable pressure gradient of 1 Pa/m is applied in all cases. Basalt density = 3000 kg/m<sup>3</sup>. Top lid of channel is allowed to move to the right at the marked speeds.

We may now exercise this equation. Let us consider first the simplest case in which there is no pressure gradient, and we are simply dragging the top plate at a speed  $U_0$  relative to the bottom plate. The second term in the equation disappears and we are left with just a linear gradient of speed connecting the two plate speeds:

$$u = U_0 \frac{z}{h} \quad (6.25)$$

The other end-member requires that there is no relative motion of the two plates, in which case the first term of equation 8 disappears. We are left with

$$u = -\frac{1}{2\mu} \frac{dP}{dx} [hz - z^2] \quad (6.26)$$

At first this looks a little disconcerting. The minus sign seems odd, until we realize that when the pressure gradient is negative, it should drive flow from left to right on the  $x$  axis. So the minus sign in fact assures us that flow moves from high to low pressure. We call  $dP/dx > 0$  an adverse pressure gradient as this drives flow in the negative  $x$  direction, whereas we call  $dP/dx < 0$  a favorable pressure gradient. What is the shape of this flow profile? It is a parabola that starts and ends at zero at the two plates.

For the more general solution we simply add the two curves (see Figure 3), meaning we are adding straight lines and parabolas, either or both of which could be negative.

### Ancillary calculations

Now that we have our flow profile, let's extract a couple interesting and important outcomes. We can for example calculate the **maximum flow speed**, the **average flow speed**, and the total flow or **discharge**. For the linear case the maximum is obviously that of the fastest plate,  $U_0$ . For the parabola, we can simply appeal to our knowledge that parabolas are symmetric about  $z=h/2$ , and evaluate the flow speed at that position. This yields:

$$u_{\max} = -\frac{1}{8\mu} \frac{dP}{dx} h^2 \quad (6.27)$$

What about the mean speed? Here we must employ the mean value theorem to calculate the mean. For this situation, this becomes

$$\bar{u} = \frac{1}{h} \int_0^h u dz = -\frac{1}{2h\mu} \frac{dP}{dx} \int_0^h (hz - z^2) dz = -\frac{1}{12\mu} \frac{dP}{dx} h^2 \quad (6.28)$$

The mean flow speed is therefore 2/3 of the maximum speed. The discharge of the flow between the plates, or the volume per unit width of the plate per unit time is simply the integral of the flow profile. We have already done that as part of the mean value theorem. As we can see from equation 12, we just need to multiply the mean flow speed by the thickness of the flow,  $h$ :

$$Q = -\frac{1}{12\mu} \frac{dP}{dx} h^3 \quad (6.29)$$

This is the so-called cubic flux law, as it relates the discharge to the cube of the flow thickness. In the next chapter we will explore application of these equations in earth sciences.

### **References**

Piau J.M., M. Bremond, J.M. Couette and M. Piau, 1994, Maurice Couette, one of the founders of rheology, *Rheologica Acta* 33:357-368.

## Applications of flow between two plates: fracture gaps, topographic ooze and salt tectonics

Now that we are armed with the theory behind the flow of a viscous fluid between two plates, let us now explore a few geological applications. These include 1) the flow of water in a narrow fracture or joint in a rock, 2) the ooze of lower crust in a channel driven by topographic gradients, and 3) the flow of a layer of halite in the subsurface, driving salt tectonics.

### *Fracture flow of water in developing karst*

Here we illustrate with a problem in which the question is how water flow through a fracture or joint network in carbonate rock leads to the evolution of cave systems. The first step in this process is evolution of the pipes that ultimately constitute a karst network. In the work of Rajaram et al. (2009) they start by considering flow within in a single fracture. If the sides of the fracture are parallel, then we are back to our flow between two plates. They then perturb the walls of the gap so that the width of the gap varies from place to place, and they calculate the dissolution rate of the walls.

In Figure 1, flow is right to left along the fracture gap that is given original random roughness. Driven by a head gradient (high on right, low on left), the flow gathers through gaps that are anomalously wide. That the flow is appropriately viewed as flow between two plates means that the flux per unit width,  $Q$ , obeys the cubic law we developed in the last chapter:

$$Q = -\frac{1}{12\mu} f(Re) \frac{dP}{dx} H^3 \quad (7.1)$$

Here  $f(Re)$  signifies a function of Reynold's number. For low  $Re$ , as we have been addressing herein,  $f(Re) = 1$ , but for high  $Re$  the function is more complicated. This formulation allows the flow to evolve naturally from a laminar flow to a turbulent flow as the gap widens and the  $Re$  increases. The novelty here is that dissolution occurs along the flow paths, allowing the gap between the rock walls to widen where dissolution is highest. This represents a feedback that ultimately localizes flow into a few dominant channels.

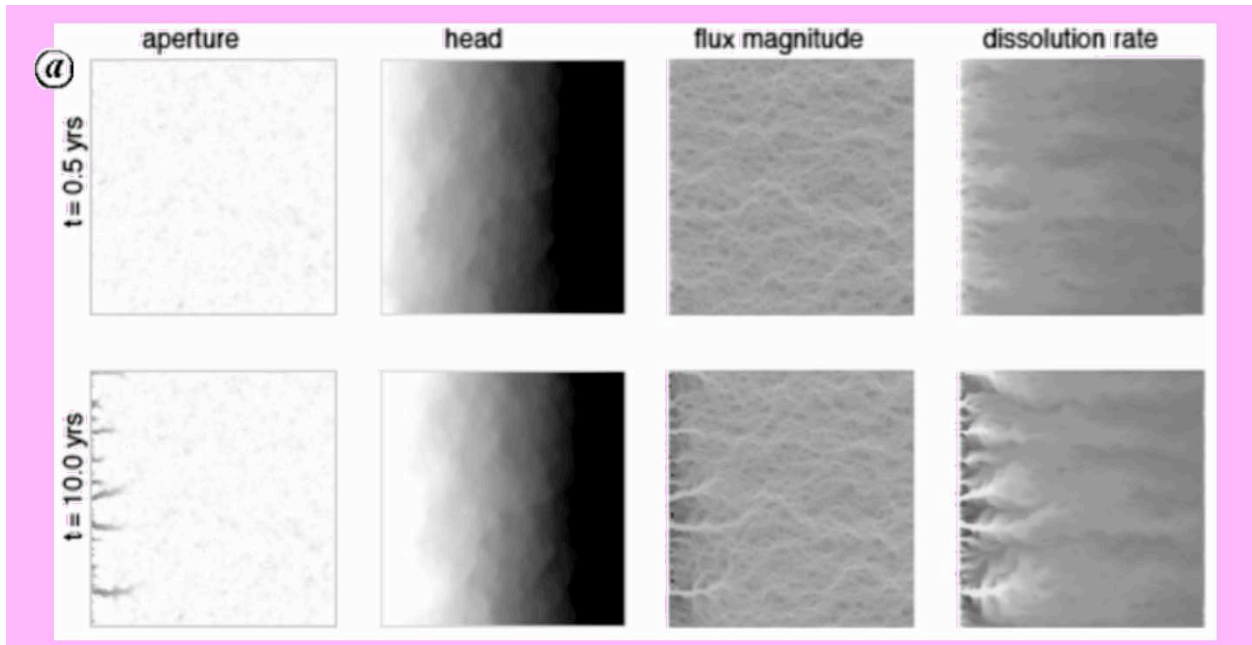


**Figure 1.** Calculations of aperture thickness, head, water flux and dissolution rate in calculation space of flow between two plates. (Rajaram et al., 2009, Figure 1)

One can see that over the 10 years simulated in this calculation, the aperture, or the local gap between the two plates, indeed widens most where the flux is highest, on the left hand side of the calculation space near the exit. Flow focuses in these wider portions of the gap, and the feedback we see initiated here is expected to increase through time to develop into discrete karst passages.

### **Topographic ooze**

In a cleverly titled *Geology* paper, “Topographic ooze: Building the eastern margin of Tibet by lower crustal flow”, Marin Clark and Leigh Royden argued that the lower crust in SE Asia basically escapes from beneath the Tibetan Plateau and accumulates outside of the plateau to produce the ramp of topography that leads smoothly southeast from the plateau toward the ocean.

Consider the present topography of the plateau and adjacent margin, and a horizontal slot or channel in the lower crust beneath it (Figure 2). In this channel the lower crust is hot enough to behave as a lower viscosity material than that either above it or below it. It is still high viscosity relative to water, say, but its relative viscosity is low enough to consider that only the material in this slot will flow. Why does it flow? Because the topography above it is tilted, meaning that the total amount of crustal material above it at the edge of the plateau is considerably higher than that above it further toward the coast. This sets up a pressure gradient directed toward ocean that should drive flow in the channel away from the plateau. Flow in a low viscosity layer is being driven by a pressure gradient established by the topography.

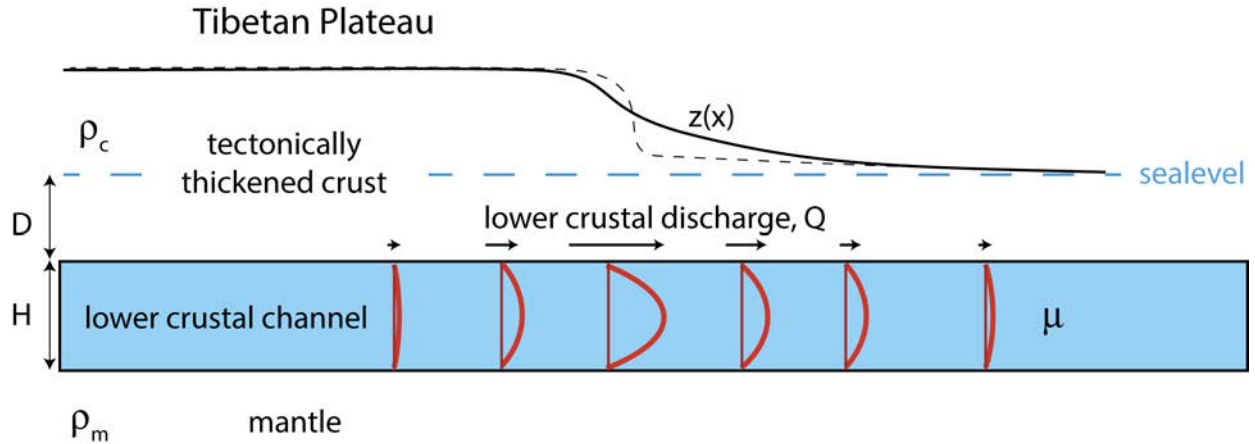


**Figure 2.** Schematic of topographic ramp leading seaward from Tibetan Plateau. Pressure gradient associated with topographic load drives flow in a low viscosity lower crustal channel of thickness  $H$ . The spatial gradients in crustal flux lead to deflation of the channel beneath the plateau edge, and inflation of the channel beyond the edge of the plateau, resulting in changes in the overlying topography.

The question is whether this process can accomplish the observed (inferred) flow in the time available, given appropriate choices for the size of the channel and the material in it. Let's set up the problem formally. The variables are shown in Figure 2. We first set up the equation representing conservation of mass for the material in the channel. The rate of thickening of the channel is governed by the spatial gradient in the flux,  $Q$ , of the lower crustal material in the channel:

$$\frac{\partial H}{\partial t} = -\frac{\partial Q}{\partial x} \quad (7.2)$$

We now appeal to the cubic flux law we have derived for flow between two plates of a material with uniform viscosity  $\mu$ :

$$Q = -\frac{1}{12\mu} \frac{dP}{dx} H^3 \quad (7.3)$$

Here the pressure  $P$  at any point reflects the overburden of crustal material:

$$P = \rho_c g(D + z) \quad (7.4)$$

where  $D$  is the depth below sealevel to the top of the channel, and  $z$  is the elevation of the surface above sealevel (Figure 2). The sum  $D+z$  is therefore the thickness of the overlying crust. If the channel is horizontal, then the pressure gradient simply mirrors the topographic gradient, as the original depth of the channel below sealevel,  $D$ , surface cancels out. Hence,

$$\frac{dP}{dx} = \rho_c g \frac{dz}{dx} \quad (7.5)$$

and we can rewrite the original equation for channel flux (volume per unit horizontal width of channel) as

$$Q = -\frac{\rho_c g}{12\mu} \frac{dz}{dx} H^3 \quad (7.6)$$

Differentiating this with respect to  $x$  and inserting in equation 2 results in an equation for the evolution of the channel thickness:

$$\frac{\partial H}{\partial t} = -\frac{\rho_c g}{12\mu} \frac{\partial}{\partial x} \left( \frac{\partial z}{\partial x} H^3 \right) \quad (7.7)$$

If we assume that the slope of the topography is entirely due to the pattern of thickening of the channel (thereby ignoring geomorphic processes), we may replace  $dz/dx$  with  $dH/dx$  to yield:

$$\frac{\partial H}{\partial t} = \frac{\rho_c g}{12\mu} \frac{\partial}{\partial x} \left( \frac{\partial H}{\partial x} H^3 \right) = \frac{\rho_c g}{12\mu} \left( \frac{\partial^2 H}{\partial x^2} H^3 + 3H^2 \left( \frac{\partial H}{\partial x} \right)^2 \right) \quad (7.8)$$

This looks downright ugly. If we take the 1<sup>st</sup> term in the big brackets to be the leading term, we recover the equation employed in Clark and Royden (2000, eqn. 4). This is a diffusion equation. If we assume that the change in  $H$  through time is small compared to the original channel thickness, the  $H^3$  may be considered essentially a constant and may be lumped with the other parameters to form a diffusivity,  $\kappa$ :

$$\frac{\partial H}{\partial t} = \left( \frac{\rho_c g H^3}{12\mu} \right) \frac{\partial^2 H}{\partial x^2} = \kappa \frac{\partial^2 H}{\partial x^2} \quad (7.9)$$

As in all diffusion problems, sharp corners will round off through time. The authors then integrate this evolution equation for a fixed period of time, and compare the resulting profiles to measured topographic profiles. They argue that this is likely to have been going on for 20 million years, and that the channel thickness is around 15 km ( $=1.5 \times 10^4$  m). It is appropriate to use average crustal density of 2600 kg/m<sup>3</sup>, and  $g = 9.8$  m/s<sup>2</sup>. Given these values, they find that the topography is well fit by a viscosity  $\mu = 10^{18}$  Pa-s for the SE-directed ramp off the plateau. This is a reasonable value given other constraints (e.g., from isostatic rebound sites, and so on).

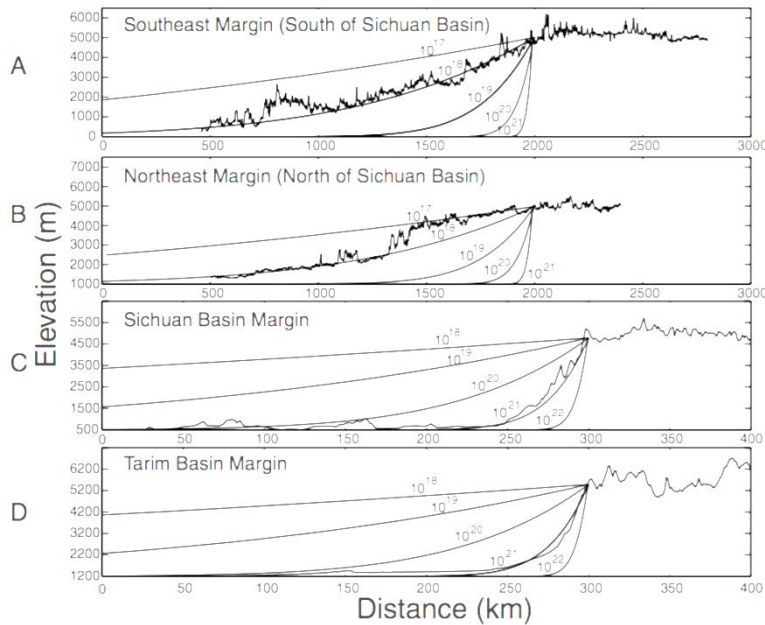
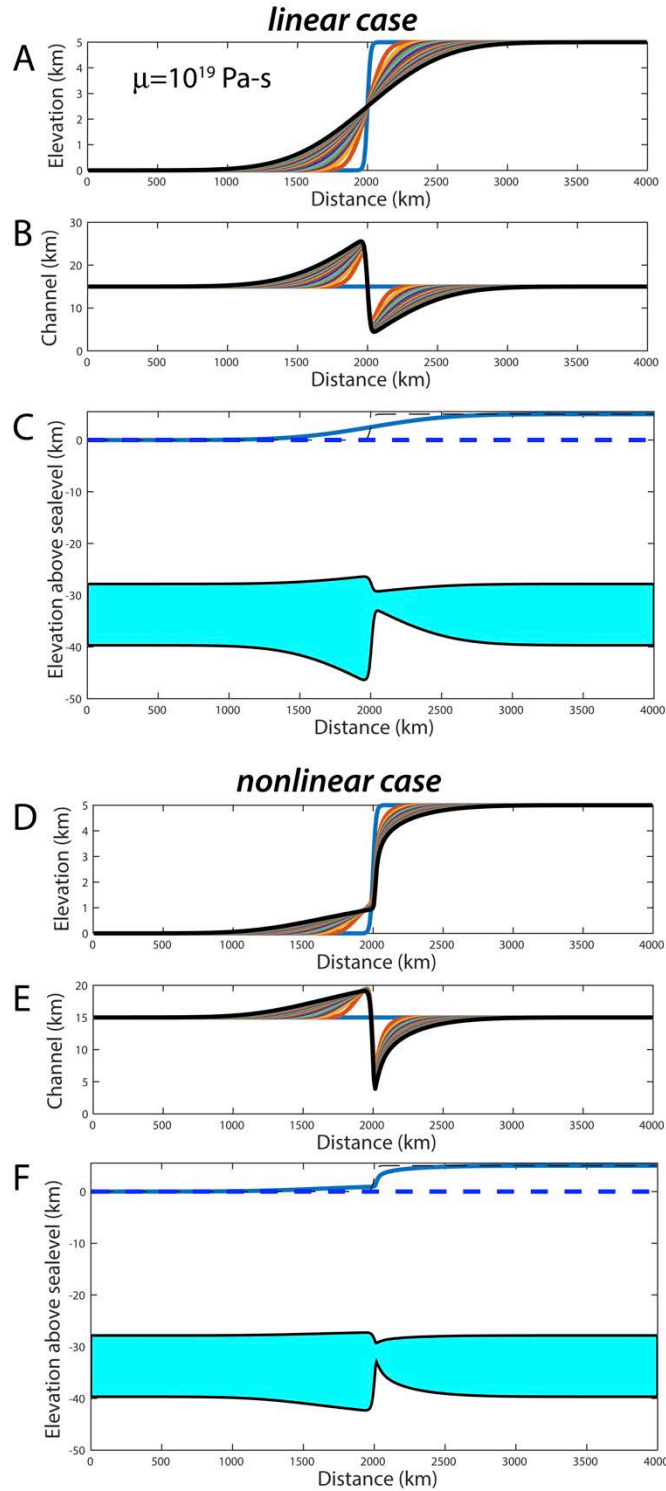


Figure 4. Model results vs. maximum topographic profiles. Model profiles represent runs for uniform lower crustal channel of thickness  $h = 15$  km and variable viscosity (labeled in Pa·s).

**Figure 3.** Observed and calculated topography on ramps beginning on the Tibetan Plateau (on right). On the SE margin of the plateau, it appears that a viscosity of  $10^{18}$  Pa-s best fits the topographic ramp. (from Clark and Royden, 2000, Figure 4)

In the above development I have short-handed a couple features of their model, such as dodging the accommodation of new topography by isostatic compensation. But the essence of the calculation is as I have presented it.

But now, for completeness, I have implemented the full equations in the calculations, and present time evolution of the ramp in Figure 4. Following Clark and Royden, I have included the isostatic compensation by multiplying the resulting topography by the ratio  $(\rho_m - \rho_c) / \rho_c$ . For the single viscosity of  $10^{19}$  Pa-s, I have run both the full nonlinear equation (eq. 7 or 8), and that implemented in Clark and Royden (equivalent to eq. 9). One can clearly see the influence of the nonlinearity associated with allowing the flux to depend on the dynamically changing thickness of the channel. The assumption that the channel thickness  $H$  is small has been violated, and the nonlinearity of the diffusion problem raises its ugly head. The response becomes distinctly asymmetrical about the position of the original topographic scarp or edge of the plateau. In the nonlinear case one can see that the thinning of the channel has greatly reduced the flux of lower crust across the edge of the plateau, so that it remains sharply defined relative to the linear case in which the thinning of the channel is prevented from playing this role.



**Figure 4.** Calculations illustrating topographic ooze through time on Tibetan Plateau edge. A-C: linear case in which changes in channel thickness  $H$  are not allowed to alter the channel discharge (equation 18). D-E: nonlinear case in which full equation for discharge is dynamic, both  $dz/dx$  and  $H^3$  changing in time. A, D: topographic profiles at 1 Ma intervals for 20 Ma, final profile in black bold line. B, E: evolving thickness of the

channel, whose initial thickness is 15 km in all calculations, shown at 1 Ma intervals. C, F: both the final topographic profile (and initial in dashed line), as well as the final lower crustal channel profile (blue fill). Most of the thickening of the channel results in drooping of the channel floor due to the implementation of full isostatic compensation at greater depths on these long time and length scales.

### *Salt tectonics*

The same physics applied to lower crustal flow in the last problem may be employed in the treatment of the flow of layers of salt in the subsurface. Here again we have an originally uniform layer of a substance capable of flow on geologic timescales, again it is subjected to pressure gradient that will drive the flow, and again the pressure gradient is established by the topography overlying the layer.



**Figure 5.** Google Earth image of the grabens in Canyonlands National Park, USA. Grabens have opened up and continue to do so due to NW-directed flow of an underlying layer of salt toward the Colorado River to the west.

Given that the problem is so parallel to that developed for the Tibetan topographic ooze, I will merely introduce a recently published (Kravitz et al., 2017) application to a local geological setting in western Colorado and eastern Utah (Figure 5). There a layer of evaporite rock, much of it halite, hundreds of meters thick was deposited in a closed basin formed in the Ancestral Rockies orogeny in the late Paleozoic. The subsequent deposition of a Mesozoic pile of rock entombed this salt. Subsequent erosion of the landscape above it during and after the Laramide orogeny has resulted in a lithostatic (rock-caused) pressure that varies from place to place. The lowest pressures occur where the Colorado River has incised deeply into the stratigraphic column overlying the salt. In places that the salt actually daylights, the pressure becomes essentially atmospheric. Just as the topographic ramp away from the Tibetan plateau establishes a pressure gradient on the underlying lower crustal channel, so too does the topographic ramp leading down to the Colorado River govern the pressure gradient driving flow of the underlying salt.

The movement of the salt can in fact be detected on the surface, as the rock is thin enough to have broken up into a series of horsts and grabens as it rides on the salt. The greater rates of flow nearest the river set up a flow gradient, which in turn results in a positive (extensile) strain rate in the overlying rock that has exceeded its tensile strength. Hence the grabens. Kravitz et al. (2017) have embraced these radar-based measurements of surface speeds (Figure 6) and have employed a numerical model to attempt to replicate the measurements. The flow in the salt is captured in algorithms that mirror the flow of a viscous substance between two plates. They treat the behavior of the overlying rock as an elastic solid that can break (Figure 7).

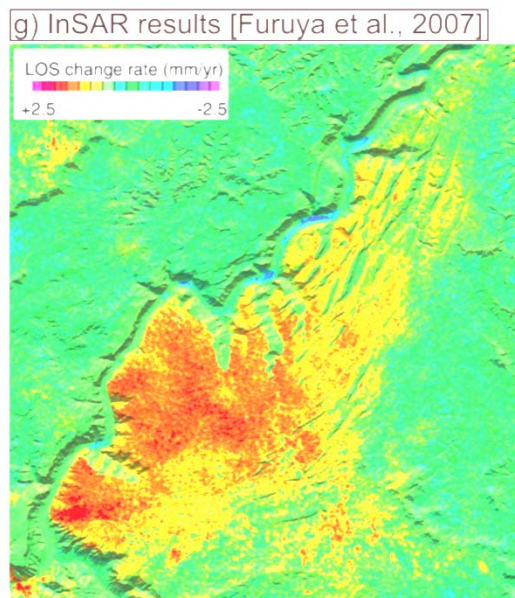


**Figure 6.** (Kravitz Figure 13g, after Furuya et al., 2007). Differential inSAR-based displacement between two images allowing surface speed estimates in mm/yr. Note rapid motion toward the Colorado River, shown as the sinuous line flowing NE-SW in its local canyon.

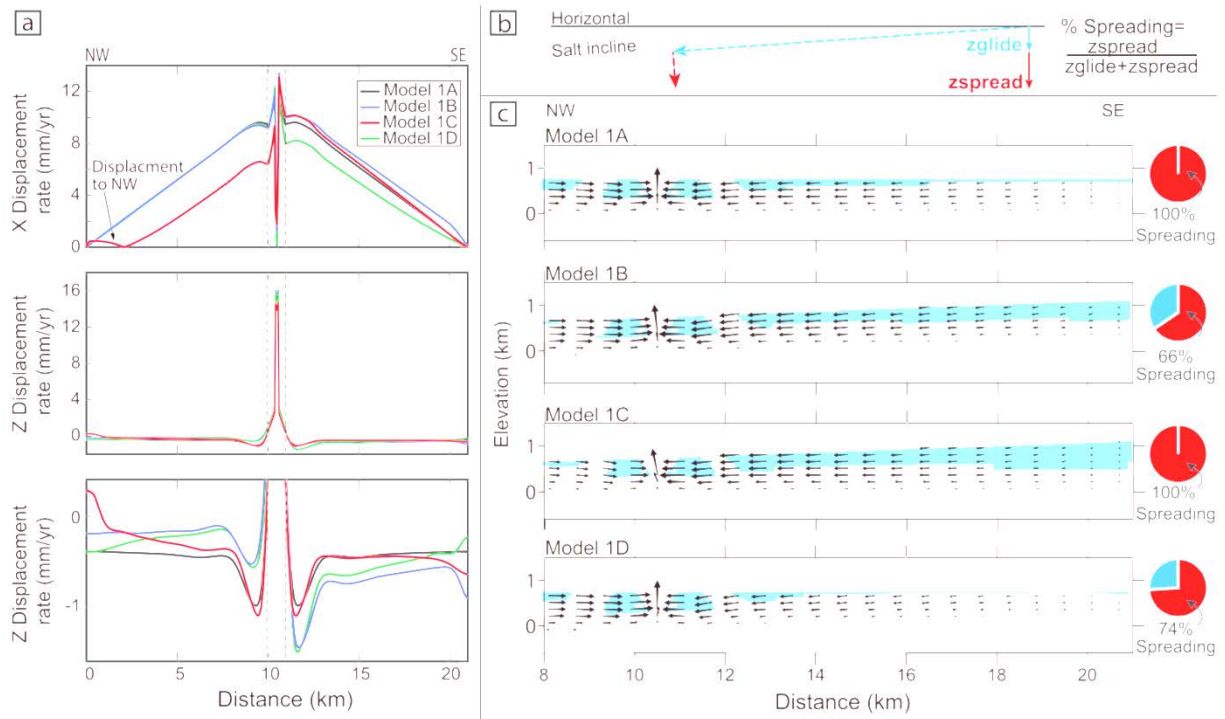


**Figure 7.** Flow vectors resulting from several model set-ups shown as models 1A-D. Salt layer is gray. In A and C the salt layer is horizontal and hence most analogous to the calculations done in the topographic ooze problem. As the overlying rock can move horizontally here (a, top panel), the simple case of flow between two plates that are both stationary is not perfectly appropriate. One can see in panel a-middle that the salt flow converges at the Colorado River (at distance = 10.5 km), which results in accumulation of salt that causes uplift of the rock, and the generation of a river anticline (and if the salt daylights, dissolution loss of the salt). (Kravitz, 2017, Figure 5)

The flow of the underlying salt layer can therefore explain several novel salt tectonic features of the topography. It can explain both the grabens as the overlying elastic rock extends, and the river anticline that parallels the river.

### Summary

In summary, we have explored several cases in which the fundamental flow of earth materials can be well captured as the flow between two parallel plates. We have seen in the first case, in which the walls are assumed to be soluble, that the flow can become turbulent as the gap between the walls widens. Rajaram et al. (2009) have incorporated a means of allowing the calculation to handle this smoothly as the Reynolds number increases. In the second case involving the edge of the Tibetan Plateau the flowing material is allowed to thicken and thin due to lateral gradients in the discharge. If this change in thickness is large enough, we can no longer assume that the thickness of the material is uniform, and the nonlinearity of the effective viscosity becomes apparent. In the case of salt tectonics, the top wall bounding the flow is neither perfectly fixed in space, and is capable of breaking up elastically. The stratigraphic package between the

top of the salt and the topographic surface is thin enough to break into blocks, which then glide with the salt.

### **References**

- Clark, M.K., L.H. Royden, 2000, Topographic ooze: Building the eastern margin of Tibet by lower crustal flow, *Geology* 28; no. 8; p. 703–706.
- Kravitz, K., P. Upton, K. Mueller, and S.G. Roy, 2017, Topographic controlled forcing of salt flow: Three-dimensional models of an active salt system, Canyonlands, Utah, *J. Geophys. Res. Solid Earth*, 122, 710–733, doi:10.1002/2016JB013113.
- Rajaram, H., Cheung, W. and A. Chaudhuri, 2009, Natural analogs for improved understanding of coupled processes in engineered earth systems: Examples from karst system evolution, *Current Science* 97(8): 1162-1176.

## Isostatic rebound

The rebound of Earth's crust in the aftermath of removal of a major load on the surface is one of our best probes of the mantle's viscosity. We develop a simple model of this problem here that banks on our knowledge of viscous flow between two plates. Consider an axially symmetric triangular deflection left in the surface by the rapid removal of an ice load (Figure 1). The triangular dent in the surface has an initial depth  $D_0$ , and we seek an expression for how this deflection  $D$  will decay with time as the mantle gooshes back under the removal site. It is measurement of this rate of change of deflection that serves as the probe of viscosity. The deflection has a total width of  $\lambda$ . The crust is uniform in thickness over the region of concern, and overlies an upper mantle with a low viscosity zone of thickness  $h$ . We will assume that the deflection recovers simply by decaying in amplitude; in other words it is at all times a triangle with width  $\lambda$  but with changing depth  $D$ .

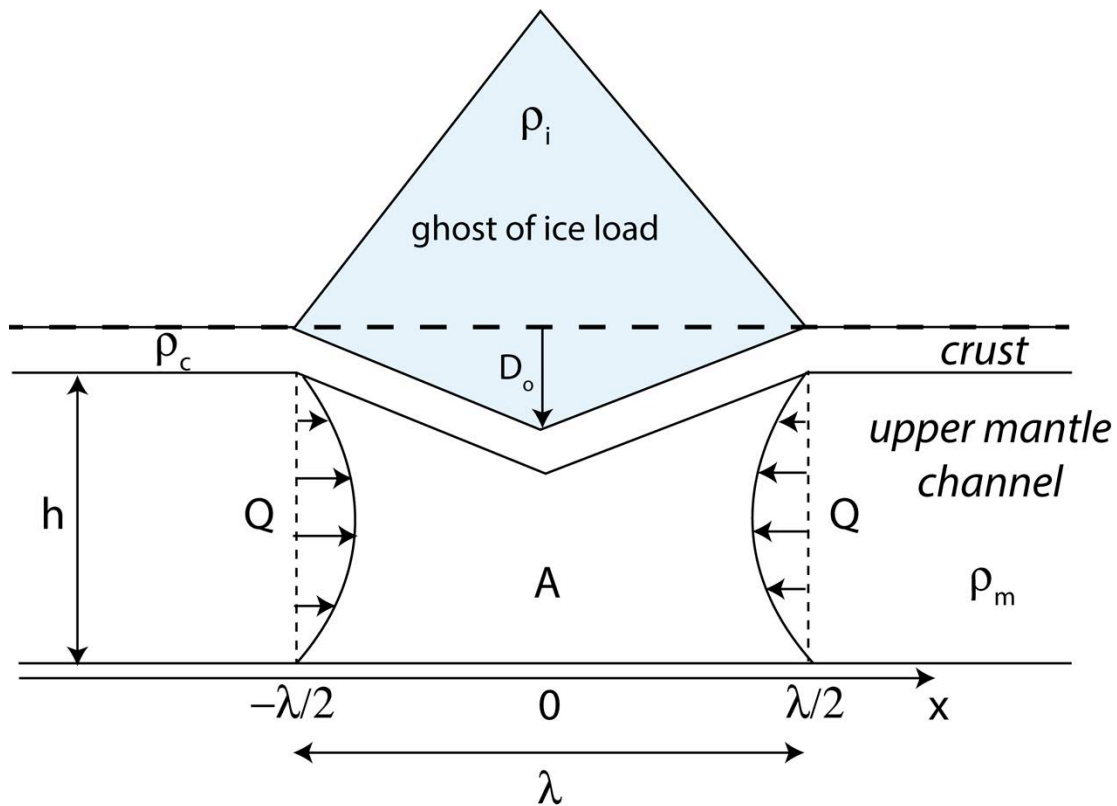


**Figure 1.** Problem set-up for consideration of rebound from removal of an ice load. Mantle response is idealized as occurring in a low viscosity channel, whose viscosity we would like to constrain from the timescale of the rebound.

We first craft an expression for conservation of mantle beneath the unloaded region, depicted by the dashed lines in the figure. Letting  $A$  be the cross sectional area of the mantle in this region, then

$$\frac{dA}{dt} = Q_{-\lambda/2} - Q_{\lambda/2} \quad (8.1)$$

where  $Q$  is the mantle discharge across the edge of the load toward the center of the unloaded region (Figure 1). We are accounting for the fact that mantle is coming from both sides toward the unloaded region. We also know that if the deflection is always triangular, then  $A = \lambda[h - (D/2)]$ . Inserting this in equation 1, and noting that the far-field channel thickness  $h$  does not change in time, yields

$$\frac{dA}{dt} = \frac{d[\lambda h - \lambda(D/2)]}{dt} = -\frac{\lambda}{2} \frac{dD}{dt} \quad (8.2)$$

We can now equate these two expressions for the rate of change of cross sectional area of mantle beneath the unloaded region, and appeal to our knowledge of the flow between two plates for an expression for the discharge  $Q$ :

$$-\frac{\lambda}{2} \frac{dD}{dt} = Q_{-\lambda/2} - Q_{\lambda/2} = \left[ -\frac{1}{12\mu} \frac{dP}{dx} \Big|_{-\lambda/2} h^3 \right] - \left[ -\frac{1}{12\mu} \frac{dP}{dx} \Big|_{\lambda/2} h^3 \right] \quad (8.3)$$

In order to proceed, we must know the pressure gradient,  $dP/dx$ , driving the flow in the channel. For simplicity let us evaluate this at the base of the mantle channel. The pressure associated with the crust is the same at the edge and the middle of the unloaded region, so this will cancel out in any evaluation of the gradient. What differs is the thickness of the mantle channel. The pressure exerted by the mantle at the edge of the load is  $P_{edge} = \rho_m g h$ , whereas that in the middle of the region is  $P_{middle} = \rho_m g (h - D)$ . And this pressure drop occurs over a distance of half the width of the unloaded region. The gradient at the right hand edge, at  $x = \lambda/2$ , is therefore

$$\frac{dP}{dx} \Big|_{\lambda/2} = \frac{P_{edge} - P_{middle}}{\lambda/2} = \frac{\rho_m g h - \rho_m g (h - D)}{\lambda/2} = \frac{2\rho_m g D}{\lambda} \quad (8.4)$$

Similarly, that at the left hand edge it is

$$\frac{dP}{dx} \Big|_{-\lambda/2} = \frac{P_{middle} - P_{edge}}{\lambda/2} = \frac{\rho_m g (h - D) - \rho_m g h}{\lambda/2} = \frac{-2\rho_m g D}{\lambda} \quad (8.5)$$

We may now insert these expressions into equation 3 to obtain our final equation for the rate of change of deflection

$$\frac{dD}{dt} = -\frac{2\rho_m g h^3}{3\mu\lambda^2} D \quad (8.6)$$

This is a first order linear ordinary differential equation for the deflection. It may be simplified by recognizing that the only thing that can change on the right hand side is the deflection  $D$ . The remaining collection of constants must have units of 1/time. Let us therefore define a characteristic timescale for the problem as

$$\tau_r = \frac{3\mu\lambda^2}{2\rho_m g h^3} \quad (8.7)$$

You should check to make sure this has units of time! Our ODE now becomes more simply

$$\frac{dD}{dt} = -\frac{D}{\tau_r} \quad (8.8)$$

This is separable, and easily solved. Taking it one step at a time, we have

$$\frac{dD}{D} = -\frac{dt}{\tau_r} \quad (8.9)$$

Integrating both sides yields

$$\ln(D) = -\frac{t}{\tau_r} + c \quad (8.10)$$

where  $c$  is a constant of integration. Recalling that our initial condition is  $D=D_o$  at  $t=0$ , we may insert these values in equation 10 to evaluate  $c$ :

$$c = \ln(D_o) \quad (8.11)$$

Subtracting this from both sides of equation 10, and recalling that  $\ln(A)-\ln(B)=\ln(A/B)$ , results in

$$\ln\left(\frac{D}{D_o}\right) = -\frac{t}{\tau_r} \quad (8.12)$$

To remove the natural logarithm we exponentiate both sides to find our final equation for the expected deflection history:

$$D = D_o e^{-t/\tau_r} \quad (8.13)$$

Let us inspect this very simple-looking equation. The deflection exponentially decays with time with a characteristic time constant of  $\tau_r$ . This means that at  $t=\tau_r$ , the deflection has decayed to  $1/e$  of its original amplitude, as shown Figure 2 below. I have also plotted the expected history of the elevation of the point in the middle of the load; as the downward deflection declines, the surface elevation increases.

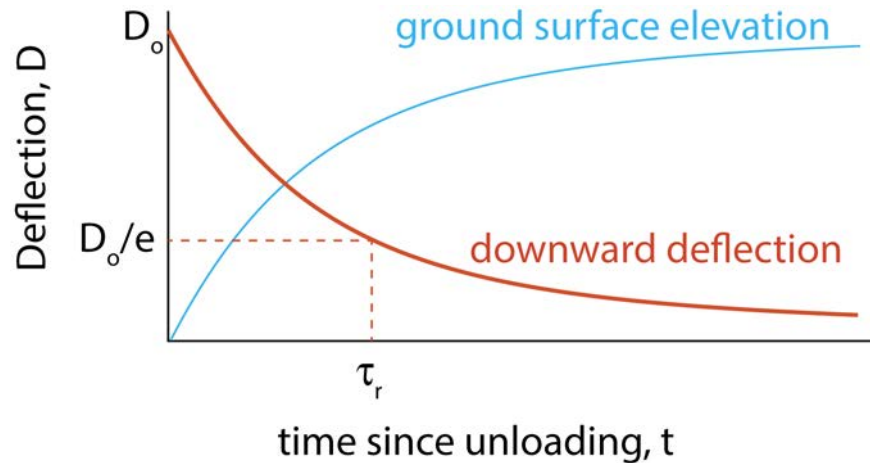


**Figure 2.** Decay of the deflection, and associated rebound of surface elevation in the aftermath of the removal of an ice load.

We now face two questions. First, what governs the initial deflection? And second, what are these characteristic response times – years? minutes? millennia? The initial deflection is governed by the deflection achieved beneath an ice load. If the ice load was left on Earth’s surface for a time that greatly exceeds this response time we are about to calculate, then it will have come into an isostatic equilibrium, which we have calculated elsewhere in this course. If the load is wide enough that it cannot be supported by flexural strength of the lithosphere, the asymptotic deflection is simply  $D_o=H_{ice}(\rho_i/\rho_m)$ , where  $H_{ice}$  is the maximum thickness of the ice, and the subscripts  $i$  and  $m$  correspond to ice and mantle, respectively. In other words, we appeal to an isostatic balance.

It remains to evaluate equation 7 to determine the response times, given realistic values of the system. But in reality, we are more likely to know or to measure the response time, and wish to back out or solve instead for the mantle viscosity. Rearranging equation 7 to solve for viscosity yields:

$$\mu = \frac{2\tau_r \rho_m g h^3}{3\lambda^2} \quad (8.14)$$

For values of response time of 4000 years, mantle channel thickness 150 km, ice load width of 500 km, and mantle density  $3300 \text{ kg/m}^3$ , we find that the mantle viscosity is approximately  $10^{19} \text{ Pa-s}$ . This is indeed a reasonable value. But I seemingly pulled this 4000 years out of my hat, right? What can we use to constrain these response times?

This is another place in the earth sciences where two sub-disciplines intersect. In this case, the constraints on the timing, which in turn can be used to place bounds on a geophysical quantity of great interest, mantle viscosity, come from raised beaches along coastlines that are rising in response to the unloading of ice. And the timing comes from dating of shells on those beaches, which is accomplished using  $^{14}\text{C}$  concentrations in the shells.

## Pipe Flow and a Model of Permeability

We now address another common example of flow in the Earth sciences: that of flow of a viscous fluid in a pipe. We would like to be able to address flow of magma through a volcanic pipe, of water through a cave passage, or of water through the connected pore space in a granular material like soil. The problem was first tackled by Jean Leonard Marie Poiseuille, a French physicist and physiologist in 1838 and by Gotthilf Ludwig Hagen, a German civil engineer. Both performed detailed experiments on pipe flow. The theory was published by Poiseuille in 1840–41 and 1846, with motivation largely that of understanding flow of blood through animal circulation systems. Laminar flow in a cylindrical pipe is often called Hagen- Poiseuille flow, or simply Poiseuille flow. In honor of Poiseuille, as of about 1913 we call the unit of viscosity in the cgs system a Poise (Sutera and Skalak, 1993).

Given the radial symmetry of a pipe, this problem is best handled in radial coordinates, with not  $x$ ,  $y$  and  $z$ , but  $r$  and  $\theta$  and  $x$ . We will not here develop the appropriate version of the Navier-Stokes equation, but instead turn to the simple problem set-up depicted in Figure 1.

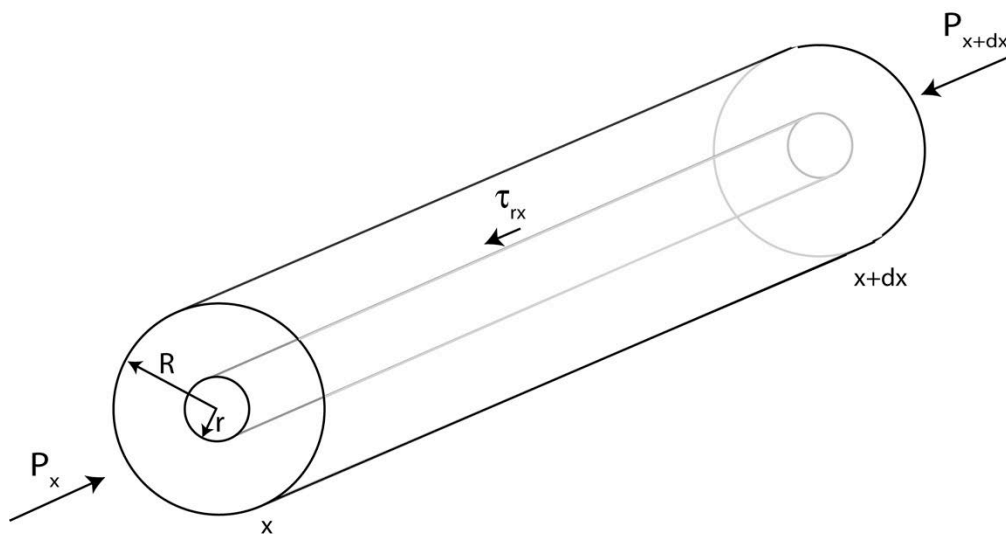


**Figure 1.** Schematic diagram for flow of a viscous fluid in a pipe of radius  $R$ . Under steady flow, the force associated with the pressure difference is balanced by the viscous forces acting along the outer edge of the tube of fluid of radius  $r$ .

Consider the element of fluid of radius  $r$  in a straight pipe of length  $dx$  and inner radius  $R$ . We wish to develop an equation for the flow profile  $u(r)$ , where  $u$  is the horizontal velocity parallel to the pipe. If (and only if) the flow is steady, we may equate the driving forces with the resisting forces. The driving forces result from any imbalance of the pressures on the fluid at each end of the fluid element, whereas the resisting forces

arise from shear stresses exerted by the adjacent layer of fluid. The pressures must be multiplied by the cross-sectional area of the element of fluid of radius  $r$  in order to represent the relevant forces. And the shear stresses exerted by the adjacent layer of fluid on the flow must be multiplied by the surface area of the tube of flow of circumference  $2\pi r$  and length  $dx$  in order to represent the resisting forces. The balance may be written:

$$P|_x (\pi r^2) - P|_{x+dx} (\pi r^2) = -\tau_{rx} (2\pi r dx) \quad (9.1)$$

Here the vertical bars signify “evaluated at” and the relevant shear stress  $\tau_{rx}$  is that acting on an  $r$  surface in the  $x$  direction. Dividing by  $dx$  and factoring out the cross sectional area of the pipe yields

$$-\tau_{rx} (2\pi r) = (\pi r^2) \frac{P|_x - P|_{x+dx}}{dx} = -\frac{dP}{dx} (\pi r^2) \quad (9.2)$$

I have appealed of the definition of a derivative in order to enact the final equality. Isolating the shear stress results in this simple relationship between the shear stress and the pressure gradient:

$$\tau_{rx} = \frac{r}{2} \frac{dP}{dx} \quad (9.3)$$

Given that the stress on the wall of the pipe is caused by viscous forces, we now appeal to the rheology of a viscous fluid to relate the shear stresses and the strain rates of the fluid. Writing Newton’s expression for the viscous stress in radial coordinates gives us

$$\tau_{rx} = \mu \frac{\partial u}{\partial r} \quad (9.4)$$

where  $\mu$  is the dynamic viscosity. Equating these last two equations, we may rearrange to find an equation for the shear strain rate:

$$\frac{\partial u}{\partial r} = \frac{r}{2\mu} \frac{dP}{dx} \quad (9.5)$$

Integrating with respect to  $r$  yields

$$u = \frac{r^2}{4\mu} \frac{dP}{dx} + c \quad (9.6)$$

We may evaluate the constant of integration,  $c$ , using the no-slip boundary condition at the inner wall of the pipe, or  $u=0$  at  $r=R$ :

$$c = -\frac{R^2}{4\mu} \frac{dP}{dx} \quad (9.7)$$

Applying this constant in equation 6 yields for the **flow profile in a pipe**:

$$u = -\frac{1}{4\mu} \frac{dP}{dx} (R^2 - r^2) \quad (9.8)$$

Note a couple features of this final result. First, the basic shape is called a paraboloid of revolution. Second, the flow moves in the positive  $x$  direction, giving a positive  $u$ , only if the pressure gradient is negative. This is as expected: flow moves from high toward low pressure.

### Ancillary calculations

As usual, let us calculate the maximum flow speed, the mean flow speed, and the discharge.

The **maximum flow speed** occurs in the center of the pipe, in the part of the flow that is furthest from the resisting walls of the pipe:

$$u_{\max} = -\frac{1}{4\mu} \frac{dP}{dx} R^2 \quad (9.9)$$

The mean flow speed is a little tricky, but we'll be tricky right back. Once we have an expression for the total pipe discharge, we can simply divide by the cross sectional area of the pipe to evaluate the mean speed. But to calculate the discharge we must acknowledge the radial symmetry of the problem. For each element  $dr$  that we are summing in the integral, the area of the flow represented by that little  $dr$  is  $2\pi r dr$  in volume. Hence the volumetric discharge, which has units of  $L^3/T$  is

$$Q = -\frac{1}{4\mu} \frac{dP}{dx} \int_0^R (2\pi r) [R^2 - r^2] dr \quad (9.10)$$

Dividing out the  $2\pi$ , distributing the  $r$ , and evaluating the integral yields

$$Q = -\frac{\pi}{2\mu} \frac{dP}{dx} \left[ \frac{r^2 R^2}{2} - \frac{r^4}{4} \right]_0^R \quad (9.11)$$

Applying the limits result in our expression for **pipe discharge**:

$$Q = -\frac{\pi}{8\mu} \frac{dP}{dx} R^4 \quad (9.12)$$

Note the extreme sensitivity to the pipe radius. The fourth power implies that a pipe twice the diameter will pass 16-fold more fluid under the same pressure gradient. We are now in a position to calculate the mean flow speed. Dividing the discharge by the cross-sectional area results in the mean flow speed:

$$\bar{u} = -\frac{1}{8\mu} \frac{dP}{dx} R^2 = \frac{u_{\max}}{2} \quad (9.13)$$

The mean flow speed is simply half of the maximum speed.

### ***Model of permeability in a granular medium as flow through small pipes***

We may now utilize the above formulas for flow in a pipe to address a fundamental problem in the earth sciences: flow of a fluid through a porous medium. This was first tackled by Darcy, who derived the following empirical relationship between the discharge of water through a porous medium, say sand, and the applied pressure gradient:

$$q = \bar{u}_d = -K \frac{dP}{dx} = -k \frac{\rho}{\mu} g \frac{dh}{dx} \quad (9.14)$$

Here I have written the specific discharge, or the Darcy velocity of the flow, the discharge of water divided by the unit cross section of a representative column of permeable granular material (which is therefore an effective mean flow speed). Let us define a few terms. The  $P$  is our familiar pressure, and hence  $dP/dx$  is the pressure gradient, and  $\mu$  is the dynamic viscosity of the fluid.  $K$  is the hydraulic conductivity,  $k$  is the permeability,  $\rho$  is the density of the fluid and  $g$  is the acceleration due to gravity. In particular, the hydraulic conductivity may be written

$$K = kg \frac{\rho}{\mu} \quad (9.15)$$

We can now see explicitly that the hydraulic conductivity reflects what planet we are on ( $g$ ), and properties of the fluid ( $\rho$  and  $\mu$ ). The remaining constant,  $k$ , the permeability, reflects properties of the medium, and it is our goal to derive a model that illuminates just what governs these properties.

Models designed to provide a physical explanation for the constant of proportionality known as the hydraulic conductivity,  $K$ , assume that flow through a porous medium may be approximated as viscous, laminar flow through a set of very small diameter tubes or pipes (see note at end for references).

We have already derived the flow speed distribution in a pipe of radius  $R$  (equation 8), and an equation for the discharge of fluid in the pipe,  $Q$  (equation 12). I re-emphasize the very strong dependence on the radius of the pipe, sometimes called the fourth-

power law for pipe discharge. The mean speed through a single pipe,  $Q/A$ , may be calculated using the diameter rather than the radius of the pipe ( $A=\pi d^2/4$ ). This is

$$\bar{u} = -\frac{d^2}{32\mu} \frac{dP}{dx} \quad (9.16)$$

While this tells us how we ought to expect the flow to go in a porous medium if it consisted entirely of a set of pipes, it does not illuminate the permeability. This requires knowledge of how these pipes are distributed within the medium. We also need to account for the tortuosity of the real flowlines. Now consider a representative volume of a soil or rock through which groundwater is being forced. A first stab at this can be taken by assuming a simple rectangular geometry in which the pipes of diameter  $d$  and length  $L$  are spaced by a distance  $D$ , representing the grain size in a soil, or the block dimension in a rock mass. This is depicted in Figure 2.

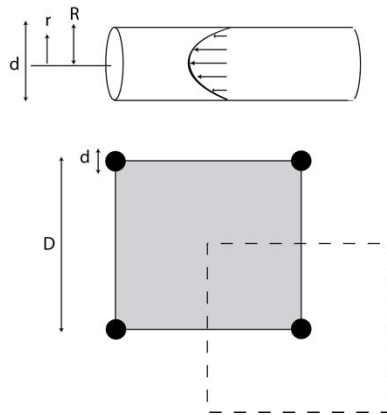


**Figure 2.** Diagram of a unit cell of width  $D$  within a granular medium. The pipes, with diameter  $d$ , at the four corners of the cell suggest that an equivalent cell (dashed) of diameter  $D$  will be served by one pipe of diameter  $d$ . We expect the flow profile within the pipe to be described by the paraboloid of revolution illustrated in the top figure. (from Anderson and Anderson, Figure 11.11)

Note that in this simple geometry we could also define the porosity, the void space divided by the total volume. A single cube contains the equivalent of one tube of length  $L$ . The porosity is then

$$\phi = \frac{[(\pi d^2 / 4)L]}{D^2 L} = \frac{\pi d^2}{4 D^2} \quad (9.17)$$

Flow through a single pipe accomplishes all of the flow contributed by a cross-sectional area  $D^2$  of the porous medium. The mean velocity across the entire volume, consisting of pipes and non-conducting masses, is, without accounting for tortuosity,

$$\bar{u}_d = -\frac{d^2}{32\mu} \frac{\pi d^2}{4D^2} \frac{dP}{dx} = -\left[\frac{\phi d^2}{32}\right] \frac{1}{\mu} \frac{dP}{dx} \quad (9.18)$$

This is equivalent to the Darcy velocity, or mean flow speed one would expect to measure through the porous medium.

Recalling equation 14 for Darcy's law, we can see that the **intrinsic permeability** of the medium may be written

$$k = \frac{C\phi d^2}{32} \quad (9.19)$$

where  $C$  is a more general (dimensionless) constant of order one reflecting the geometry of the connected pore space. Permeability has units of area ( $\text{cm}^2$ ,  $\text{mm}^2$ ...)

This development allows us to see that the hydraulic conductivity,  $K$ , combines descriptors of the fluid ( $\rho/\mu$ ) and descriptors of the medium ( $\phi d^2$ ) through which the fluid is passing. Defining the permeability serves to isolate the properties of the medium. The porosity of a soil does not vary greatly - perhaps tens of percent. We therefore expect that permeability will go as the square of the pore diameters in a soil. One might imagine that the pore diameters ought to scale as the grain size.

Let us try an example. Consider clean sand with diameter 0.2 mm. Its pore diameters might then be 0.1 mm or  $10^{-2}$  cm. If the sand also has a typical bulk porosity of 0.3, we calculate its intrinsic permeability from equation 19 to be about  $10^{-6}$   $\text{cm}^2$ . This is in the ballpark according to the table reproduced in Figure 3. Our very simple model of permeability not only captures the observed strong dependence on grain size of the medium, but puts us in the right order of magnitude. This is encouraging.

Note: This development of a permeability model is taken closely from Anderson and Anderson, *Geomorphology*, chapter 11. That development in turn follows discussion in Turcotte and Schubert, 2002; Furbish, 1997; and Freeze and Cherry, 1979, following Hubbert, 1940.

**Table 2.2 Range of Values of Hydraulic Conductivity and Permeability**

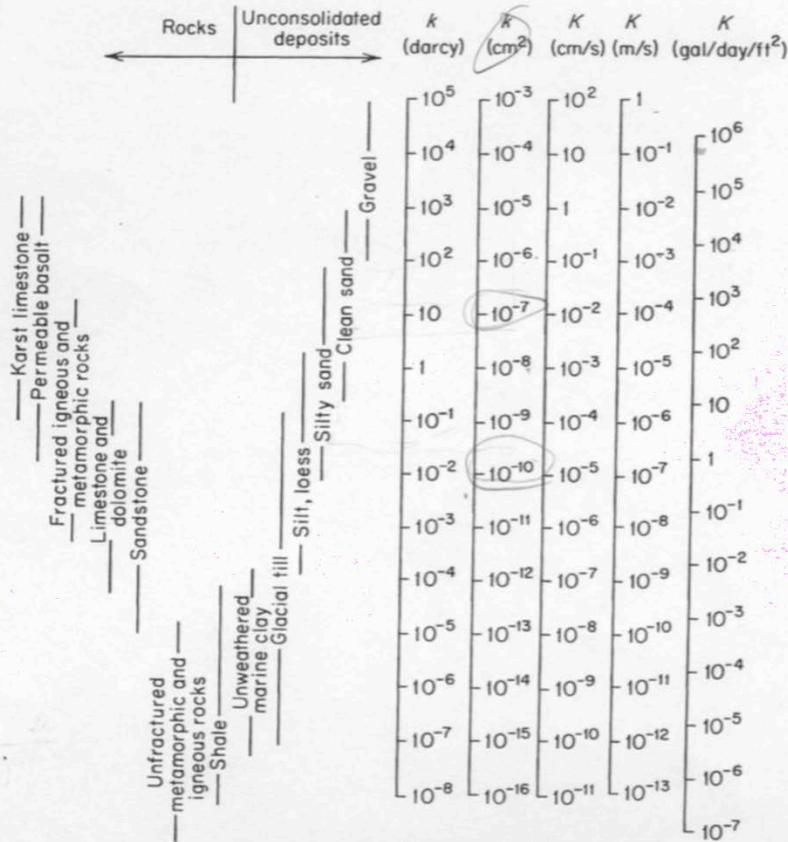


**Table 2.3 Conversion Factors for Permeability and Hydraulic Conductivity Units**

	Permeability, $k^*$			Hydraulic conductivity, $K$		
	cm <sup>2</sup>	ft <sup>2</sup>	darcy	m/s	ft/s	U.S. gal/day/ft <sup>2</sup>
cm <sup>2</sup>	1	$1.08 \times 10^{-3}$	$1.01 \times 10^8$	$9.80 \times 10^2$	$3.22 \times 10^3$	$1.85 \times 10^9$
ft <sup>2</sup>	$9.29 \times 10^2$	1	$9.42 \times 10^{10}$	$9.11 \times 10^5$	$2.99 \times 10^6$	$1.71 \times 10^{12}$
darcy	$9.87 \times 10^{-9}$	$1.06 \times 10^{-11}$	1	$9.66 \times 10^{-6}$	$3.17 \times 10^{-5}$	$1.82 \times 10^1$
m/s	$1.02 \times 10^{-3}$	$1.10 \times 10^{-6}$	$1.04 \times 10^5$	1	3.28	$2.12 \times 10^6$
ft/s	$3.11 \times 10^{-4}$	$3.35 \times 10^{-7}$	$3.15 \times 10^4$	$3.05 \times 10^{-1}$	1	$6.46 \times 10^5$
U.S. gal/day/ft <sup>2</sup>	$5.42 \times 10^{-10}$	$5.83 \times 10^{-13}$	$5.49 \times 10^{-2}$	$4.72 \times 10^{-7}$	$1.55 \times 10^{-6}$	1

\*To obtain  $k$  in ft<sup>2</sup>, multiply  $k$  in cm<sup>2</sup> by  $1.08 \times 10^{-3}$ .

**Figure 3.** Table of permeabilities,  $k$ , and hydraulic conductivities,  $K$ .

**References**

Sutera, S. P. and R. Skalak, 1993, The history of Poiseuille's law, *Annual Reviews of Fluid Mechanics* 25: 1-19.

## Steady Uniform Flow of a Viscous Fluid in an Open Channel

Many flow problems relevant to the earth sciences are what we term open channel flows. They contain no top lid, and are open to the atmosphere that does not exert any stress on the fluid. Here we seek the equation for the vertical profile of horizontal velocity,  $u(z)$ , in the case of a steady uniform flow down an inclined plane. The slope of the plane with respect to the horizontal is  $\theta$ , the thickness of the flow  $h$ , and the fluid has a uniform viscosity  $\mu$ .

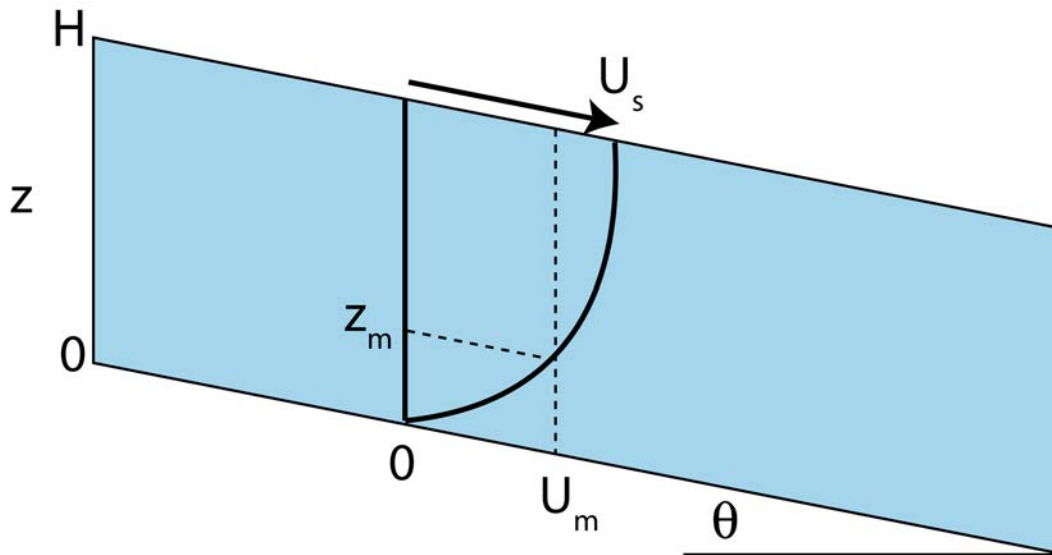


**Figure 1.** Schematic diagram for open channel flow down an inclined plane. Profile of flow  $U(z)$  is shown, with  $z$  taken positive upward.  $U_s$  is surface velocity, and  $U_m$  is the vertically averaged velocity, which may be measured at a height  $z_m$  above the bed.

### *Simplifying the Navier-Stokes equation for the problem at hand*

We must take the  $x$ -component of the Navier-Stokes equation and solve it for the particular flow situation.

$$\frac{\partial u}{\partial t} + u \frac{\partial u}{\partial x} + v \frac{\partial u}{\partial y} + w \frac{\partial u}{\partial z} = g_x - \frac{1}{\rho} \frac{dP}{dx} + \nu \frac{\partial^2 u}{\partial x^2} + \nu \frac{\partial^2 u}{\partial y^2} + \nu \frac{\partial^2 u}{\partial z^2} \quad (10.20)$$

These are the assumptions and how they impact the Navier-Stokes equation:

- The flow is steady. This allows us to set all derivatives with respect to time to zero. The first term on the left hand side (LHS) vanishes.
- The flow is horizontally uniform. This allows us to ignore terms with gradients in  $x$  and  $y$ . The 2<sup>nd</sup> and 3<sup>rd</sup> terms on the LHS vanish, and the second derivatives with respect to  $x$  and  $y$  vanish on the right hand side (RHS).

- The flow is entirely driven by the downslope component of gravity, hence  $g_x = g \sin(\theta)$ . The pressure gradient may be assumed to be negligible, as the flow thickness is uniform in the channel. The second term on the RHS vanishes.
- There is no flow through the bottom of the channel, in either direction, into or out of the bed. This requires that the vertical velocity of the flow vanish at the boundary, meaning  $w = 0$  at  $z = 0$ . From continuity in an incompressible medium, we know that  $\frac{\partial u}{\partial x} + \frac{\partial v}{\partial y} + \frac{\partial w}{\partial z} = 0$ . Horizontally uniform conditions require that the 1<sup>st</sup> two terms vanish, leaving  $\frac{\partial w}{\partial z} = 0$ . Integrating this yields  $w = \text{constant}$ . The boundary condition of no flow through the boundary allows us to assess this constant to be zero. Since  $w = 0$  everywhere, the last term on the RHS=0. Hence the entire LHS of the equation = 0.

Given these assumptions, the x-component of the N-S equation then simplifies to

$$\nu \frac{d^2 u}{dz^2} = -g_x \quad (10.21)$$

This is an ordinary, linear 2<sup>nd</sup> order differential equation. The left hand side captures the effect of diffusion of momentum by viscosity, whereas the right hand side represents a source of momentum, here through the body force. Note that this looks identical in form to the case of flow between two plates driven by a pressure gradient. Using the definition of the kinematic viscosity, it may be rewritten:

$$\mu \frac{d^2 u}{dz^2} = -\rho g_x \quad (10.22)$$

### **Solving for the flow profile**

To obtain the equation for the flow profile,  $u(z)$ , we will have to integrate twice. For laminar flow in which the  $Re \ll 1$ , and in which the temperature is uniform so that the viscosity can be taken to be uniform, we may divide both sides by viscosity and integrate the equation to obtain an equation for the gradient of the velocity

$$\frac{du}{dz} = -\frac{\rho g \sin(\theta)}{\mu} z + c_1 \quad (10.23)$$

Here  $c_1$  is a constant of integration. In an open channel flow, we may safely assume that the velocity gradient vanishes at the top of the flow, as there is no overlying fluid exerting a shear stress on the fluid in the channel. Therefore at  $z=h$ ,  $du/dz = 0$  and

$$c_1 = \frac{\rho g \sin(\theta)}{\mu} h \quad (10.24)$$

Integrating once more yields

$$u = \frac{\rho g \sin(\theta)}{\mu} \left( hz - \frac{z^2}{2} \right) + c_2 \quad (10.25)$$

where  $c_2$  is our second constant of integration. This we evaluate knowing that the flow speed goes to zero at the boundary (the no-slip boundary condition), in which case  $c_2$  vanishes and we have for our final flow velocity profile

$$u = \frac{\rho g \sin(\theta)}{\mu} \left( hz - \frac{z^2}{2} \right) \quad (10.26)$$

This is the solution for a steady low  $Re$ , laminar flow velocity profile in an open channel. It is a parabola, just as in the flow between two plates driven by a pressure gradient. But here we take only the bottom half of the parabola.

### Ancillary calculations

Now that we have our flow profile, let us again extract a few important formulas. We will calculate the **maximum flow speed**, the **average flow speed**, and the integral of the flow or **discharge**.

The maximum speed ought to occur at the top of the flow, at  $z=h$ . Evaluating equation 7 for  $z=h$  yields

$$u_{\max} = \frac{\rho g \sin(\theta)}{2\mu} h^2 \quad (10.27)$$

As we did with the Couette case, we may employ the mean value theorem to obtain the mean velocity:

$$\bar{u} = \frac{1}{h} \int_0^h u dz = \frac{\rho g \sin(\theta)}{h\mu} \int_0^h \left( hz - \frac{z^2}{2} \right) dz = \frac{\rho g \sin(\theta)}{3\mu} h^2 \quad (10.28)$$

Comparing the mean and the maximum, we see that the mean speed is 2/3 of the maximum speed, just as it was in the parabolic flow between two plates.

The discharge in an open channel is then simply the product of the mean speed and the flow depth, yielding

$$Q = \frac{\rho g \sin(\theta)}{3\mu} h^3 \quad (10.29)$$

The discharge goes as the cube of the flow thickness. Double the thickness of the flow and the discharge increases 8-fold.

But there is one more instructive calculation we can carry out in this situation. If you were to be asked to make one measurement of flow velocity to capture the mean speed of the flow, at what depth into the flow, or at what height above the bed, would you make that measurement? This can be solved by finding at what height  $z=z_m$ , in equation 7 one finds the mean speed from equation 9. Given that the  $\frac{\rho g \sin(\theta)}{\mu}$  cancels out, we are left with

$$hz_m - \frac{z_m^2}{2} = \frac{h^2}{3} \quad (10.30)$$

We wish to solve this for  $z_m$ . Lo and behold this is a quadratic in  $z_m$ , and we can use the quadratic formula we memorized in middle school. Remember  $x = -b \pm \sqrt{b^2 - 4ac}$  all over  $2a$ ? We'll use that here. Rearranging equation 11 into the proper form, we see that

$$\frac{z_m^2}{2} - hz_m + \frac{h^2}{3} = 0 \quad (10.31)$$

Using  $a = 1/2$ ,  $b = h$ , and  $c = h^2/3$  we obtain

$$z_m = h \left( 1 \pm \sqrt{1/3} \right) \quad (10.32)$$

Knowing that the mean speed ought to be measured within the flow rather than above it means we should take the minus sign rather than the plus sign, which yields  $z_m = 0.42h$ . The mean speed would be measured  $4/10^{\text{th}}$  of the way from the base of the flow to the top, or  $6/10^{\text{th}}$  of the way from the top toward the bed.

Indeed, this is a rule of thumb used by the USGS to measure the mean speed of water in a channel. I note that the flow in a real channel in the field will in fact be turbulent, and our equation breaks down for turbulent flows. Nonetheless, when one employs the same strategy for this calculation for the turbulent case, using what is called the law of the wall velocity profile, we obtain something very close to this, and one can defend the practice of measuring the flow speed at  $6/10^{\text{th}}$  of the way toward the bed from the flow top.

## Glaciers as examples of open channel flow

While it may not seem that glaciers are appropriate examples of open channel flow, one may in fact consider the often U-shaped valleys in which they flow to be their channels. What makes them different from what we have discussed so far is that their rheology is not linear but is instead non-linear. Here we tackle that particular feature and explore the degree to which this makes them different from linear viscous flows.

Recall that the linear viscous rheology we appealed to in these problems is that in which there is a linear relationship between the strain rate of the fluid and the stress to which it is subjected. That is, when we “closed” the force balance represented by Cauchy’s first law to arrive at the Navier Stokes equations, we employed the relationship:

$$\frac{\partial u}{\partial z} = \frac{1}{\mu} \tau_{zx} \quad (11.1)$$

This is plotted in Figure 1. But there are other materials that do not conform to this linear relationship, but instead are described by,

$$\frac{\partial u}{\partial z} = A |\tau|^{n-1} \tau_{zx} = A \tau_{zx}^n \quad (11.2)$$

where  $A$  is called the flow law parameter, and  $n$  the power. This represents a general rheological description in which the strain rate goes as some power,  $n$ , of the stress.

John Glen (1952) performed experiments on ice soon after WWII, and discovered that ice was better fit with a non-linear relationship, one in which  $n$  was not 1. Please see his descriptions of the experiments, beautifully archived in the British Library oral history: <https://sounds.bl.uk/Oral-history/Science/021M-C1379X0026XX-0002V0>

Glen’s data were best fit with a 4<sup>th</sup> power in the high stress domain, and a first power (linear) in the lower stress domain (Figure 2). This has most often been summarized as a third power, or cubic, relationship, forcing a fit through all of the data. The case for  $n=3$  is now called Glens flow law. The first expression in equation 2 is most general, where  $\tau$  is the total stress to which the material is subjected, but for our purposes, in which the only stress being applied is the shear stress,  $\tau_{zx}$ , the final expression will suffice. The point is that the relationship is no longer linear. This too is plotted in Figure 1, and original data and Glen’s plotting of it are reproduced in Figure 2.

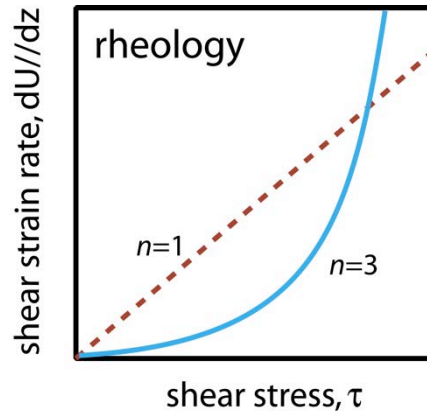


Figure 1. Plots representing the rheology of two materials: linear rheology (dashed red,  $n=1$ ) and non-linear fluid (solid blue, here  $n=3$ ) are shown. Ice behaves as an  $n=3$  fluid.

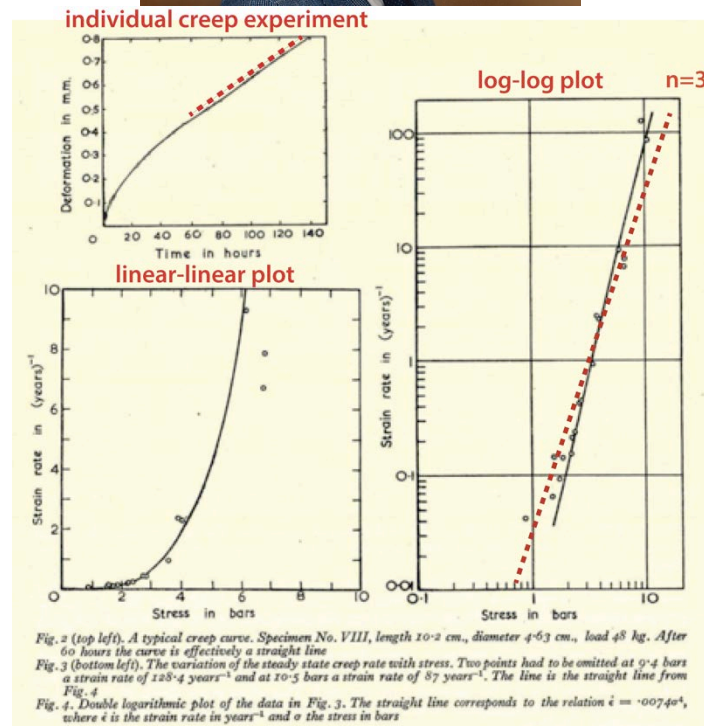


Figure 2. top) Photo of John Glen when interviewed by the British Library. bottom) Reproduction of John Glen's (1952; Figures 2-4) initial experiments on polycrystalline ice, with my annotations in red. The straight line fit on the log-log plot in his Figure 4 has a slope of 4, hence argues for a 4<sup>th</sup> power in the rheological law for the creep of ice. If the low-stress points are included, one can imagine a lower slope of 3 better fits the entirety of the data (my added red dashed line). This plot defines what we now call Glen's flow law for ice.

But let me give you a little historical context. The interest in the rheology of ice was not entirely driven by the academic pursuit of the study of glaciers. Indeed, it was stimulated by engineering issues that arose during WWII associated with this zany idea: how to build an aircraft carrier out of ice, what the British called a “bergship”. And Churchill demanded that Nature would be allowed to aid in the construction as much as possible. As well summarized in the first issue of the *Journal of Glaciology* (Perutz, 1948), construction of such “monsters” of ice were thought to provide an alternative to aircraft carriers required to allow planes at the time (1941), with their limited range, to be supported from close enough to their bombing targets. They required a landing strip of 600 m length. While experiments on icebergs had shown that they crack when blasted by shellfire and torpedos, the addition of only a few percent of wood pulp was sufficient to prevent the cracking. As the inventor of the wood pulp-ice mix was a fellow by the name of Pyke, and the material produced was similar to concrete, this material became known as pykrete. Deformation experiments on pykrete showed that it shared a material behavior similar to metals in which it deformed at a measurable (although low) rate under a prescribed load, and that this rate likely depended upon temperature. This behavior required a certain type of reinforcement of the void envisioned in the design of the bergship, as the walls would deform under their own weight (Figure 3). Although the bergship project was ultimately abandoned as island-hopping in the Pacific became more efficient, the ranges of planes increased, and the landing strip length increased beyond the original design, the further understanding of the deformation of pure ice was stimulated by this effort. This became John Glen’s research project, carried out in the basement of the Cavendish laboratory at Cambridge, at the same time that Watson and Crick were working.

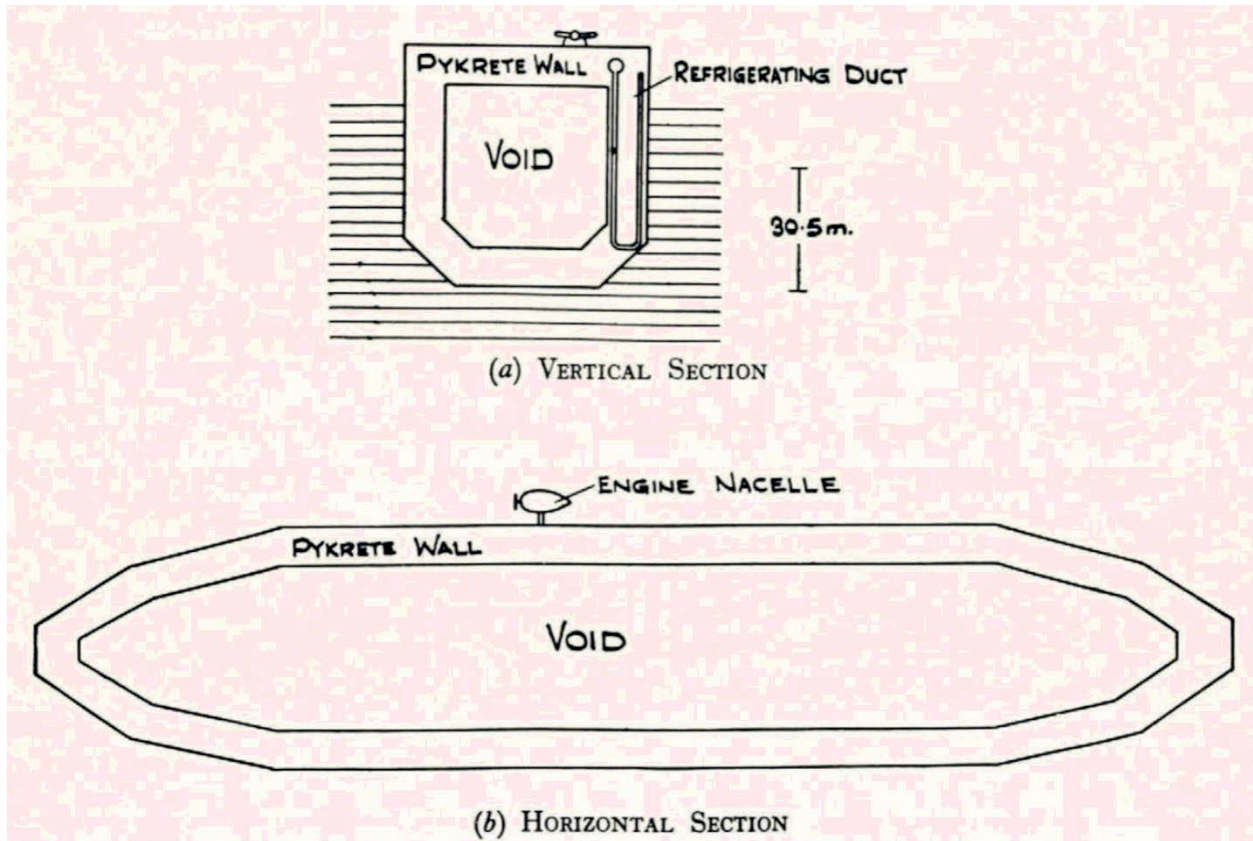


Figure 3. Diagrams of the bergship design that stimulated experiments on ice. Top: cross-section showing aircraft atop the flight deck, the structure of which was to be constructed of “pykrete”, a mix of wood pulp and ice. Bottom: plan view. Length of the ship needed was greater than 800 m. (Perutz, 1948, Figure 3)

By rearranging equation 2 to look like equation 1, we can define an “effective viscosity”,  $\mu_{eff}$ , that sits in the place of viscosity in equation 1.

$$\frac{\partial u}{\partial z} = \frac{1}{\mu_{eff}} \tau_{zx} = \frac{1}{\frac{1}{A\tau_{zx}^2}} \tau_{zx}; \mu_{eff} = \frac{1}{A\tau_{zx}^2} \quad (11.3)$$

The effective viscosity depends upon the stress, and in particular, the effective viscosity declines rapidly as stress increases. What does this mean? To assess this, we have to recall what the stresses look like in a glacier. They increase linearly toward the bed, from zero at the top surface of the ice, to a maximum at the bed.

Because the stresses are high near the bed, the ice there behaves like a much weaker, less viscous, more runny fluid than the ice at the top of the glacier. Think about how that will alter the velocity profile. Let us now follow this through in deriving the expected velocity profile in a glacier.

The stress profile within the glacier is as we saw in the last chapter:

$$\tau_{zx} = \rho_i g(H - z)S \quad (11.4)$$

It increases linearly to a maximum at the bed. We may now insert this expression into equation 2 for the profile of strain rate:

$$\frac{du}{dz} = A[\rho_i g(H - z)S]^3 \quad (11.5)$$

Integrating this with respect to  $z$  results in the velocity profile:

$$u = A(\rho_i gS)^3 \left\{ H^3 z - \frac{3}{2} H^2 z^2 + H z^3 - \frac{1}{4} z^4 \right\} \quad (11.6)$$

The dependence on the thickness of the ice,  $H$ , is much stronger in this case than in the linear case, with terms that go as the 4<sup>th</sup> rather than the 2<sup>nd</sup> power. As can be seen in Figure 4, the change in velocity near the bed is significantly more abrupt than in the parabolic profile of the linear viscous case. The flow is much more plug-like in the interior of the ice. The strain rate, the rate of change of the velocity with height above the bed, is much higher in the glacier case than in the linear viscous case.

### *Ancillary calculations*

We now seek expressions for the maximum speed, the mean speed, and the discharge of ice. In all cases, the nonlinearity of the flow law will result in a much stronger dependence on the flow thickness.

The maximum speed is found by evaluating equation 6 at  $z=H$ , the surface of the glacier:

$$u_{surf} = A(\rho_i gS)^3 \frac{H^4}{4} \quad (11.7)$$

Note two things: the surface speed of the ice, which one could measure with GPS, or with repeated surveys of stakes on the ice surface, goes as the fourth power of the ice thickness. Double the ice thickness, and the surface speed should increase by 2<sup>4</sup> or 16-fold. And the surface speed increases as the cube of the surface slope.

The ice discharge is the full integral of the ice speed from bed to surface. By integrating equation 6 and evaluating it from 0 to  $H$  results in:

$$Q = A(\rho_i gS)^3 \frac{H^5}{5} \quad (11.8)$$

and the mean speed is the ice discharge divided by the thickness, or

$$\bar{u} = A(\rho, gS)^3 \frac{H^4}{5} \quad (11.9)$$

Note that the mean speed is 2/3 of the surface speed in the linear viscous case, and 4/5 of the surface speed in the cubic flow law case. For power law rheologies, the general expression is  $\bar{u} = u_{surf} \left[ \frac{n+1}{n+2} \right]$ . Recall here that the  $n=1$  case is in fact our original Newtonian linear viscous case.

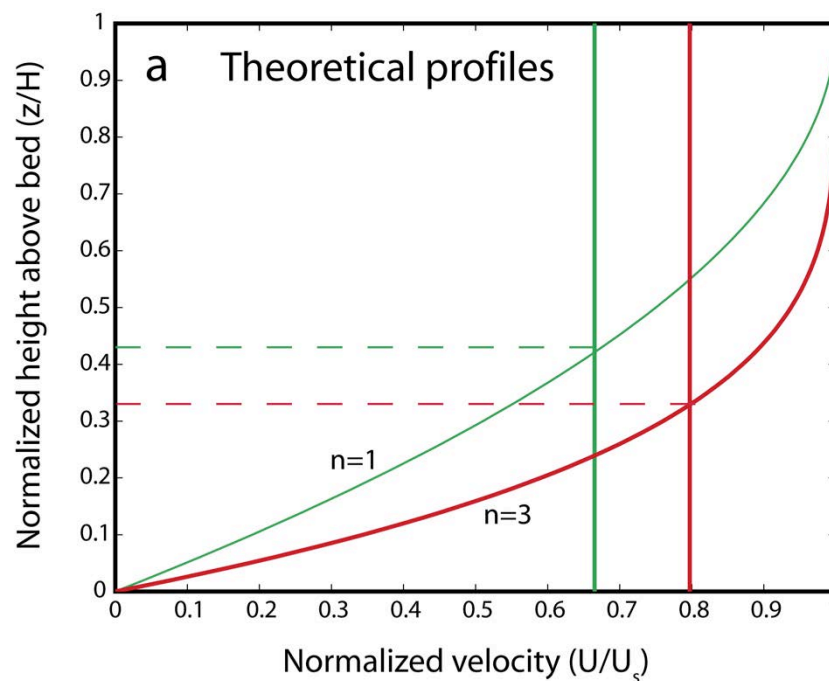


Figure 4. Flow profiles for  $n=1$  (green) and  $n=3$  (red) fluids, normalized against maximum height above bed and maximum flow speed. The mean speed is shown as the vertical lines, and the position above the bed at which this mean speed would be measured is signified by the dashed horizontal lines. As the nonlinearity of the rheology increases, the mean speed approaches the surface speed, and the depth at which it would be measured is found nearer the bed. (after A&A Figure 8.11)

So, what does this mean? How does this nonlinearity of the flow law or rheological law affect a glacier's behavior? One of the implications is that a glacier does not have to change its thickness much to alter the discharge of ice a lot. For example, a 10% increase in thickness will accomplish 1.1<sup>5</sup> or 60% increase in discharge.

## References

- Anderson, R.S. and S.P. Anderson, 2010, **Geomorphology: The Mechanics and Chemistry of Landscapes** (Cambridge University Press) textbook, 640 pp., published June 2010.
- Cuffey, K.M., and Paterson, W.S.B., 2010, **The Physics of Glaciers**. 4th edition. Academic Press (704 pp).
- Glen, J.W., 1952, Experiments on the deformation of ice, *Journal of Glaciology* 2 (12): 111–114.
- Perutz, M.F., 1948, A description of the iceberg aircraft carrier and the bearing of the mechanical properties of frozen wood pulp upon some problems of glacier flow. *Journal of Glaciology* 1 (3): 95- 104.

## Settling of particles in fluids

Any object falling under the influence of gravity will accelerate until the drag force opposing its motion is equal to the force pulling it downward, the weight of the particle. At this point, the vertical speed no longer increases, and the object is said to be at its fall velocity (also called its *terminal velocity* or *settling velocity*). This balance is an example of Newton's law of motion, which states that the acceleration of an object is equal to the sum of the forces acting on it and is inversely proportional to the mass of the object. We have all memorized this as  $F = ma$ . By the time the object hits the ground, it has achieved its fall velocity, which means that the acceleration in this familiar equation  $a = F/m$  is zero. This condition occurs when  $F = F_{drag} + F_w = 0$ , where  $F_{drag}$  is the drag force acting on the object, and  $F_w$  is its buoyant weight.

We note that this weight should be the buoyant weight, in general. In the case of a raindrop or a quartz particle settling in air, the weight of the displaced fluid (air) is trivial relative to that of the object, and may be neglected. Since  $F_w$  and  $F_{drag}$  act in opposite directions, they have opposing signs, and the fall velocity is reached when their magnitudes are equal. Here we will focus on objects that are spherical.

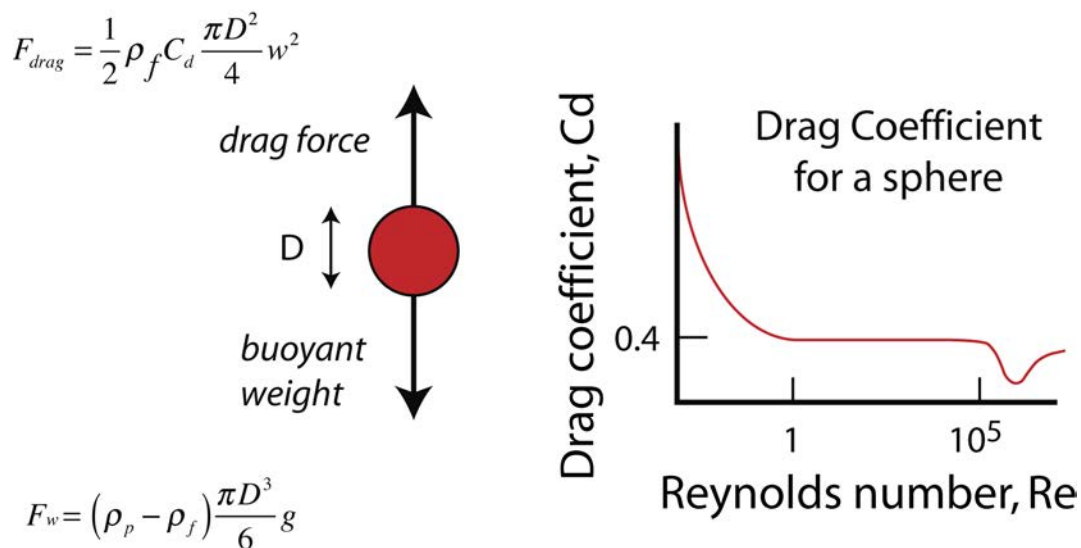


**Figure 1.** Problem set-up showing (left) a sphere with both body force (buoyant weight) and opposing drag force and (right) the relationship between the drag coefficient,  $C_d$ , and the Reynolds number,  $Re$ .

The force balance on a sphere is illustrated in Figure 1. The vertical coordinate,  $z$ , is taken to be positive downward, and, as is common in fluid mechanics, we call the vertical velocity  $w$ . The only acceleration in this case is in the vertical, meaning that we can write the acceleration of our spherical object to be the rate of change of the vertical speed, or  $dw/dt$ . The buoyant weight acts downward, in the negative  $z$  direction, and may be written as

$$F_w = M_b g = (\rho_p - \rho_f) V_p g = (\rho_p - \rho_f) \frac{\pi D^3}{6} g \quad (12.1)$$

where  $\rho_p$  and  $\rho_f$  are the density of the particle and of the fluid, respectively. In the last equality we have employed the formula for the volume of a sphere of diameter  $D$ .

The opposing force acting to retard the fall, the drag force, is a little more complicated, as it depends strongly upon the speed of the object relative to the fluid. In general we might expect the drag force to represent the product of the surface stresses or pressures imposed by the fluid with the surface area of the particle. A representative area of the particle is its cross-sectional area, and a representative stress is the pressure that we may write as  $\rho_f w^2$ . One may therefore write a general formula for the drag force as

$$F_{drag} = \frac{1}{2} \rho_f w^2 \frac{\pi D^2}{4} C_d \quad (12.2)$$

where  $C_d$  is a non-dimensional parameter called the *drag coefficient*, and in general  $w$  is the vertical speed of the particle relative to the fluid (if the fluid is still, this is simply the speed of the particle). This drag coefficient is dependent upon the speed of the object; in fact it depends upon whether the flow around the object is laminar or turbulent, which is captured by the Reynolds number,  $Re$ . This is only one of the many non-dimensional numbers one encounters in fluid mechanics problems. This particular number represents the relative importance of inertial forces and viscous forces in the problem. The dependence of the drag coefficient upon the Reynolds number is shown in Figure 1. Ignoring the little dip out there at very high  $Re$  (a feature dubbed the drag crisis, at  $Re$  of  $\sim 2 \times 10^5$ ), there are essentially two asymptotic expressions -- one at very high  $Re$ , the other at low  $Re$ . At high  $Re$ , the drag coefficient becomes a constant, at 0.4. And at low  $Re$ , the drag coefficient is inversely dependent upon  $Re$ , following the relationship  $C_d = 24/Re$ . In short then,

$$\begin{aligned} \text{for } Re < 1, C_d &= 24 / Re = \frac{24v}{wD} \\ \text{for } Re > 10, C_d &= 0.4 \end{aligned} \quad (12.3)$$

The transition region between these two end-members is captured well by a piecewise equation tabulated by Morsi and Alexander (1972). The general expression for the vertical acceleration of the particle is given by the sum of  $F_w$  and  $F_{drag}$ , both divided by the mass of the object (i.e.,  $a = \Sigma F/M$ ):

$$\frac{dw}{dt} = \left( \frac{\rho_p - \rho_f}{\rho_p} \right) g - \frac{3 \rho_f C_d}{4 \rho_p D} w^2 \quad (12.4)$$

Here the first term represents the acceleration due to the body force of gravity, the second represents the opposing acceleration caused by fluid drag. To determine the settling velocity, which by definition occurs when the weight is exactly balanced by the

drag force, we simply set the left hand side of equation 4 to zero, apply the relevant formula for the drag coefficient from equation 3, and solve the resulting equation. This results in two expressions for settling velocity, one for low and the other for high Reynolds numbers:

$$\text{for low Re: } w = \frac{gD^2(\rho_p - \rho_f)}{18\mu} \quad (12.5)$$

$$\text{for high Re: } w = \sqrt{\frac{gD(\rho_p - \rho_f)}{0.3\rho_f}} \quad (12.6)$$

If you are doing such a calculation, you should check to make sure you have chosen the correct formulation of the drag coefficient, by assessing the  $Re$  associated with the calculated settling velocity. If you used the low  $Re$  formulation, and find  $Re \gg 1$  for the calculated settling velocity, or vice versa, you have used the wrong formulation. In Figure 2 we show the fall velocities for objects of several densities in both water and air, calculated using a fuller representation of the  $C_d(Re)$  function that spans the transition region between low and high Reynolds numbers (see Morsi and Alexander, 1972). One may also turn to a very simple formulation that incorporates both end-members and is quite accurate in between (Ferguson and Church, 2004).

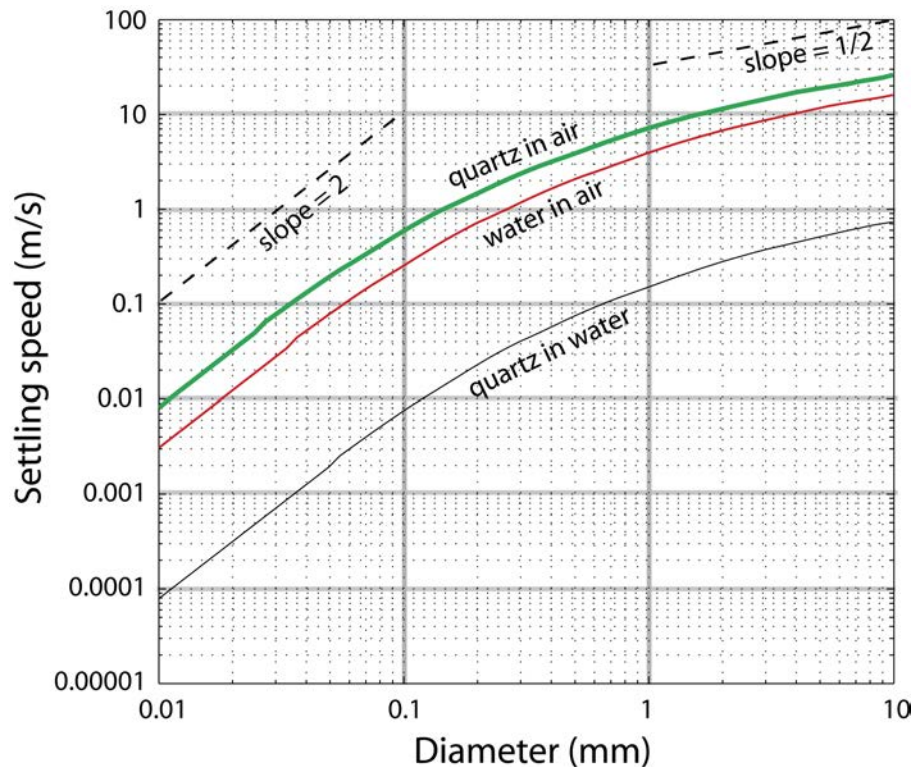


**Figure 2.** Settling speeds as a function of particle diameter, for three cases: water droplets in air, quartz in air, and quartz in water. Note the square root dependence on  $D$  for small sizes and speeds, and the  $D^2$  dependence for large sizes and speeds.

The bottom line is that for small particles the settling speed increases as the square of the particle diameter, whereas for larger particles it increases as the square root of the diameter. Let's make sure that we can all interpret this graph. I have stated that the dependence for low  $Re$  is a squared relationship. On a log-log plot as presented in Figure 2, the slope of the line is the power in the power law. The slope for low  $Re$  is about 2 (you go up by two decades for every decade across). And the predicted slope at high  $Re$  is the opposite: you go up one decade for every two decades across, for a slope of  $1/2$ .

### Response times

Let's dig just a little deeper into just how a particle will react to being dropped into a fluid. We seek to know how long it will take to achieve this settling speed, a time we will call the *response time*. In equation 7, I have taken the drag coefficient to be the low  $Re$  formula, and have simplified the acceleration equation to become:

$$\frac{dw}{dt} = \left( \frac{\rho_p - \rho_f}{\rho_p} \right) g - \frac{18\rho_f\nu}{\rho_p D^2} w = A - Bw \quad (12.7)$$

In the last equality I have collected all terms that do not change in time to be constants  $A$  and  $B$ . This reduces our equation to a simple linear ordinary differential equation – linear because no term involves squares of variables or their derivatives, first order because the highest derivative is the first. I note that the constant  $B$  must have units of  $1/\text{time}$ , and furthermore that this time is the time to reach  $1/e$  of the asymptotic value,  $A/B$ , which is equivalent to the settling speed (see Figure 3). So the characteristic response time in the problem is therefore

$$T_r = \frac{\rho_p D^2}{18\rho_f\nu} = \frac{\rho_p D^2}{18\mu} \quad (12.8)$$

At least this is appropriate for the low  $Re$  case used to arrive at equation 7. It is worth proving to yourself that this expression indeed has units of time.

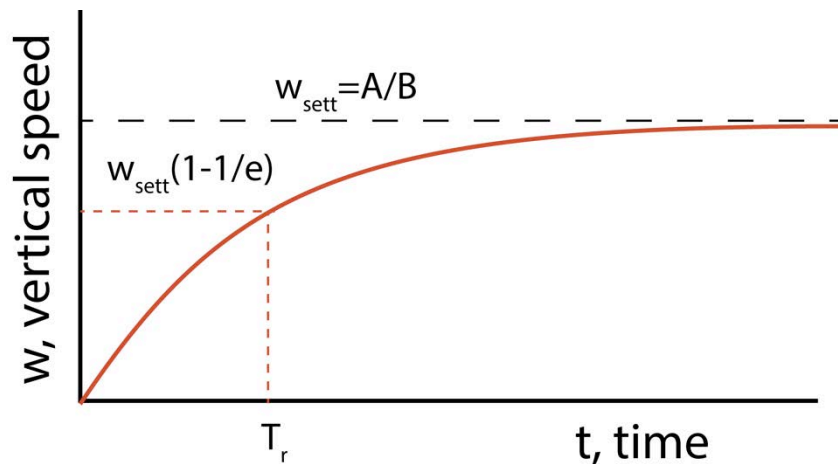


**Figure 3.** Vertical speed history of a falling sphere, showing both the asymptotic or settling speed, and the characteristic response time of the system.

Let's work a couple examples.

I. For a typical 0.1 mm raindrop falling in air, the response time is  $T_r = 0.03$  s. If dropped from a dropper, it would take 0.03 seconds to reach  $1-1/e$  of its settling speed, or perhaps 0.1 s to reach its full settling speed. This is relevant for example if we wish to perform experiments to assess the efficacy of rainsplash in moving sediment. For a 1 mm droplet, the time will be significantly longer, and we would have to erect quite a tall apparatus if we wish the drops to reach their settling speed before impact! Can you calculate how tall it would have to be?

II. For quartz of diameter 0.1 mm in air (fine sand typical of dunes), we find  $T_r = 0.12$ s. This is longer than most hops in eolian saltation, meaning that the trajectory will not have enough time to respond to fluctuations in wind speed, and hence will be smooth (not wiggly). We dub such trajectories to be *saltation* rather than *suspension*. Particles half or a tenth this size (very fine sand and silt) will respond significantly to fluctuations by the time they should land, and hence will be wiggly and hence are likely to be "suspended".

Note: much of this chapter is derived from the hillslopes chapter in Anderson and Anderson (2010).

### References

- Anderson, R.S. and S.P. Anderson, 2010, *Geomorphology: The Mechanics and Chemistry of Landscapes* (Cambridge University Press) textbook, 640 pp., published June 2010.
- Anderson, R.S. and Hallet, B., 1986, Sediment transport by wind: Toward a general model. *Geological Society of America Bulletin* 97: 523-535.
- Anderson, R.S., 1987, Eolian sediment transport as a stochastic process: The effects of a fluctuating wind on particle trajectories. *Journal of Geology* 95: 497-512.
- Dietrich, W.E., 1982, Settling velocity of natural particles. *Water Resources Research* 18: 1615–1626.
- Ferguson, R.I. and M. Church, 2004, A simple universal equation for grain settling velocity. *Journal of Sedimentary Research* 74: 933–937.
- Morsi, S.A. and A.J. Alexander, 1972, An investigation of particle trajectories in two-phase flow systems. *Journal of Fluid Mechanics* 55: 193–20.

## The Speeds of Tectonic Plates

The motion of lithospheric plates in plate tectonics is a manifestation of the convection of the Earth's mantle. Indeed, one can think of the mantle as being driven by heavy plates falling within the mantle. This outer half of the planet is being both cooled from above, and heated from below. Just as a pot of soup heated from below will ultimately convect, moving hot soup up from below and cold soup from the surface downward, so too will a body of rock heated and cooled under the proper conditions. Likewise, just as a lake cooled from above in the fall will ultimately "turn over", moving cold surface water down to the bottom, so too will the mantle. Both bottom-up and top-down forcing can drive convection (see Davies' (1999) wonderful chapters on this). The cooling occurs ultimately through radiation of heat to outer space, and is dictated essentially by the great difference in temperature between the Earth's surface and outer space. The heating at the base of the mantle is caused by its contact with the very rapidly convecting liquid iron of the outer core. Heat moves into the mantle from the core by conduction; it is also lost from the mantle to the atmosphere and the ocean by conduction through the lithosphere. The regions within which conduction reigns as the heat transport mechanism are called conductive boundary layers. They are each on the order of a few tens to 100 km thick; the energy transport in the remaining part of the 2900 km thick mantle is dominated not by conduction but by convection – by the transport of heat by the moving material.

Convection can occur whenever the forces driving overturn of a fluid are greater than those resisting such motion. In most general terms, the force promoting convection is buoyancy, which is scaled by the density difference between the one portion of the fluid and another, and by how big this blob of anomalous fluid is. The density difference can arise from either compositional or thermal effects. In the case of mantle convection, thermal effects dominate. The force resisting this motion scales with the viscosity of the fluid, and with the surface area of the anomalous blob. It is common to derive a ratio of driving to resisting forces that may be used to characterize whether or not convection should occur, and how vigorous the convection might be. This ratio, which is dimensionless, is called the Rayleigh number, denoted  $Ra$ . When this Rayleigh number is above about 2000, convection driven by thermal buoyancy should occur. For the Earth's mantle, the Rayleigh number is presently on the order of  $10^5$ , meaning that it ought to be convecting quite vigorously.

Given this physics, how fast ought plates to be moving in the Earth mantle system? Can we, from first principles, predict the rates at which the plates are moving across the Earth's surface? Given that plate tectonic speeds determine the pace of mountain building events, which drive rock above sea level where terrestrial erosive surface processes can attack it, and generate topographic gradients that dictate the rates of geomorphic processes, this is a crucial number. In addition, note that if we have a theory that allows calculation of these rates, we will be in a position to evaluate

quantitatively how these rates might have been different in the past, when the Earth was younger and perhaps even more vigorously convecting.

Here I explore a model in which the plate tectonic engine is driven from the top, with speeds governed by the rate of fall (or settling) of dense cold rigid lithospheric plates into the mantle below. The problem may be reduced to a force balance. If we assume that the plates are not accelerating, in other words that they are moving at the same rate today as they were last year as they were hundreds of years ago, which is probably a safe assumption, then the forces that are driving them must be in balance. This is a simple restatement of Newton's second law:  $F = ma$ , where  $F$  is the sum of the forces operating to cause motion,  $m$  is the mass of the object, and  $a$  is the acceleration. The object of concern is a lithospheric plate. We simply have to identify the forces acting on the plate, and equate them, as shown in Figure 1.

The problem is akin to a settling problem with which we are more familiar, except that the object that is settling is not a sphere, but a slab. The forces operating are  $F_b$ , the (negative, downward) buoyant force of the slab, caused by its having a density that is slightly higher than the remainder of the mantle, and  $F_r$ , the (positive, upward) resisting force, caused by viscous drag along the surface of the slab as it descends through the very viscous mantle. Our task is to estimate the magnitude of each of these terms and set them equal (so that their vector sum is zero). First, we need an equation for the buoyancy force. Let's consider a unit thickness of mantle (into the page), in which case we need expressions for the force per unit width. If the thickness of the mantle is  $D$ , and the horizontal length of the convecting cell is also  $D$  (a crude approximation), then the buoyant force per unit width of slab pulling it downward is

$$F_b = D\delta g(\rho_l - \rho_m) \quad (13.1)$$

where  $\delta$  is the thickness of the lithosphere upon subduction,  $g$  is the acceleration due to gravity, and  $\rho_l$  and  $\rho_m$  are the lithospheric and mantle densities, respectively. We can see that the force increases linearly with the thickness of the slab upon subduction.

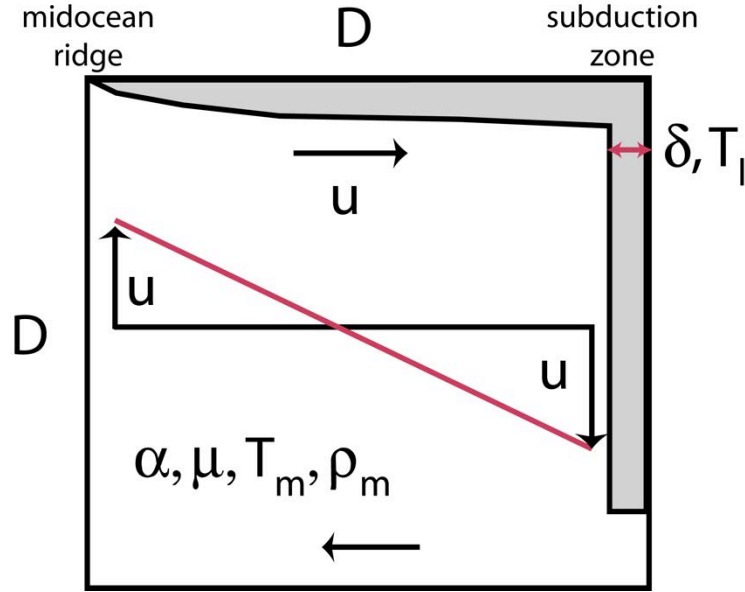


**Figure 1.** Convection in a box. Base of the box is the core-mantle boundary. Width of the box is a half-ocean basin. We wish to know the plate speed,  $u$ . Material properties, temperatures, and thickness of the lithosphere upon subduction are noted. (after Anderson and Anderson, 2010, Figure 3.8)

The resisting force is a drag force, or a surface traction, that operates on the surfaces of the slab. This requires knowledge of the shear stress (a force per unit area) and the area over which it operates. Given that we are doing a balance on only a 1m sliver into the page, the area really translates to the length of the boundary between mantle and lithosphere, or  $2D$ . If we assume that the rheology of the mantle is a linear viscous one, then the shear stress is the product of the viscosity of the deforming material,  $\mu$ , here the mantle, and the rate at which it is straining, or the shear strain rate,  $\partial u / \partial r$ . In other words,

$$F_r = 2D\tau = 2D\mu \frac{\partial u}{\partial r} \quad (13.2)$$

where  $r$  is the distance from the center of the mantle. Here the shear rate is the rate at which the velocity within the mantle changes with distance away from the lithosphere (see Figure 1). The whole mantle cell is turning over with a speed of  $u$  at its perimeter means that while the right hand side is going down at  $u$ , the left side is coming up at  $-u$ . The difference,  $2u$ , occurs over a distance of  $D$ , meaning that  $\partial u / \partial r = 2u/D$ . The resisting force is therefore

$$F_r = 2D\mu \frac{2u}{D} = 4\mu u \quad (13.3)$$

Equating the buoyant driving and the resisting forces per unit length, and solving for the unknown velocity, results in

$$u = \frac{D\delta g(\rho_l - \rho_m)}{4\mu} \quad (13.4)$$

The thicker and longer the lithospheric slab, the faster it will settle into the mantle, whereas the higher the viscosity the lower its speed will be.

But we are not done. We must still calculate the thickness of the lithosphere, and the density difference between lithosphere and mantle. The lithosphere thickens by conduction, which is controlled by the thermal diffusivity,  $\kappa$ , and the time since cooling at the surface began – i.e. since it left the mid-ocean ridge. In particular, the thickness at the site of subduction is

$$\delta = \sqrt{\kappa T} = \sqrt{\kappa(D/u)} \quad (13.5)$$

where  $T$  is the time it takes for the lithosphere to move from spreading center to subduction zone,  $D/u$ . Note that the faster the lithosphere moves, the thinner the lithosphere will be by the time it subducts. We have also discussed the density difference between lithosphere and mantle, as we needed this number in order to evaluate the isostatic balance and the bathymetric profile of the ocean basin. The density difference is simply

$$\Delta\rho = \rho_l - \rho_m = \alpha\Delta T \rho_m \quad (13.6)$$

where  $\Delta T$  is the difference in temperature between the lithosphere and the surrounding mantle. This leaves us with the following equation for the speed of the plate:

$$u = \frac{Dg\alpha\Delta T \rho_m \sqrt{\kappa D/u}}{4\mu} \quad (13.7)$$

Noting that  $u$  is involved in the thickness of the lithosphere, we multiply both sides by the square root of  $u$ , and then take the 2/3 root of both sides to arrive at our final equation for plate speed:

$$u = \left( \frac{g\alpha\Delta T \rho_m \sqrt{\kappa}}{4\mu} \right)^{2/3} D \quad (13.8)$$

We are now in a position to estimate the expected modern plate speed. We need to estimate all of these variables. What is the temperature difference between mean mantle and mean lithosphere? Given that the surrounding mantle is vigorously convecting and hence does not vary greatly from that at the base of the lithosphere, we can take its temperature to be that of the base of the lithosphere. The mean temperature of the lithosphere is well approximated by the average of its top and its base, given that the thermal profile within the lithosphere is crudely linear. Hence,  $\Delta T = 1200 - ((1200 - 0)/2) = 600^\circ\text{C}$ . The other variables may be taken to be:  $D = 2900 \text{ km} =$

$2.9 \times 10^6 \text{ m}$ ,  $g = 10 \text{ m}^2/\text{s}$ ,  $\rho_m = 3.3 \times 10^3 \text{ kg/m}^3$ ,  $\kappa = 1 \text{ mm}^2/\text{s} = 10^{-6} \text{ m}^2/\text{s}$ ,  $\mu = 10^{22} \text{ Pa-s}$ , and  $\alpha = 3 \times 10^{-5}/^\circ\text{C}$ . The resulting estimate of plate speed (really the half-spreading rate, because the lithosphere on the other side of the spreading ridge is moving away at the same speed) is  $2 \times 10^{-9} \text{ m/s}$ , or  $0.06 \text{ m/yr}$ , or  $6 \text{ cm/yr}$ . We have already documented actual plate speeds, which are a little slower than this. Typical convergence rates are more like  $5\text{-}10 \text{ cm/yr}$ , and hence  $2.5\text{-}5 \text{ cm/yr}$  for expected half-spreading rates. Given the necessarily crude estimates of the values of the parameters, we have come astonishingly close to reality! The answer to our original question of whether we can predict the speeds of plates from first principles is a resounding yes.

It is also instructive, before we leave this calculation, to inspect the final equation for the velocity, and assess how this might have changed through geologic time. Among all these variables, what is likely to have changed? Physical constants like  $g$  and  $\alpha$  and  $\kappa$  certainly will not have changed. The variable that is most susceptible to change is the viscosity of the mantle. The viscosity of a material is highly dependent upon temperature. In particular, it declines greatly with increasing temperature, exponentially so. If the mantle in early times were significantly warmer than it is now, then the viscosity would have been much lower. Note how the viscosity enters the equation for the plate speed:  $u \sim \mu^{-2/3}$ . If the viscosity were an order of magnitude (10 times) lower in the early Earth, then the plate speed would have been  $(1/10)^{-2/3}$  or 4.6-fold faster then. It is a good thought experiment to explore the implications of this for the topography of the early Earth.

As discussed in Davies (chapter 5), this allows us to calculate expected cycling times in the mantle. It would take a parcel of mantle a time of  $4D/u$  to traverse the circuit around our box. At speeds we have calculated (and measured) for the present, using  $D = 2900 \text{ km}$ , and  $u = 6 \text{ cm/yr}$ , yields a cycle time of  $190 \text{ Myr}$ . Given that the planet is  $4.5 \text{ billion years old}$ , the mantle will have had plenty of time to be stirred. It would indeed have performed  $4500/190$  or  $24$  cycles. This is a minimum number of cycles, given our argument above that the speeds would have been higher when the mantle was warmer in an early Earth. We therefore expect that the chemistry of the mantle would be relatively homogeneous, much as a marbled vanilla and chocolate cake batter becomes if you stir it too much – rather than discrete swirls of black and white, it becomes a dull and uninteresting gray.

Note: much of this development is presented in the Large-scale topography chapter in Anderson and Anderson (2010).

## References

- Anderson, R.S. and S.P. Anderson, 2010, *Geomorphology: The Mechanics and Chemistry of Landscapes* (Cambridge University Press) textbook, 640 pp., published June 2010.
- Davies, G., 1999, *Dynamic Earth: Plates, Plumes and Mantle Convection*, Cambridge: Cambridge University Press.
- Oxburgh and Turcotte, D.L., 1967, Finite amplitude convection cells and continental drift, *J. Fluid Mech.*, 28, 29-42, 1967.

Turcotte, D.L. and G. Schubert, 2002, *Geodynamics*, 2nd edition, Cambridge: Cambridge University Press.

# Convective Instabilities and Mantle Plumes

## *Examples of instability problems*

Nature commonly exhibits patterns that arise automatically in a particular system. In many cases, we see that tiny wiggles in a system's behavior organize themselves into a pattern in which one wavelength dominates. The tiny wiggles we call perturbations. If a perturbation grows, it is said that the system is unstable with respect to perturbations. If it decays or dies away, it is said that the system is stable against perturbations.

We are familiar with many examples. To name a couple, ripples inevitably evolve in sand when the wind blows across it, and the ripples are commonly about 10 cm in wavelength. Convective clouds dot the summer sky with kilometer spacing.

In stability analyses, we ask these two questions: Under what conditions does the perturbation grow vs damp? What is the fastest growing of the possible perturbations? It is this fastest growing perturbation that will likely be the one that wins out and dominates the problem, or in other words this perturbation dictates the spatial length scale.

Here we will explore the stability of the lower boundary of the mantle, and ask under what circumstances the base of the mantle heated from below by the hot iron core will give rise to mantle plumes.

I note that the treatment below follows closely that in Davies' books (1999, 2011) on plume instability, which I highly recommend.

## *Part I. Plumes from the core-mantle boundary*

Consider the problem sketched in Figure 1. The very lowermost portion of the mantle is a thermal boundary layer within which the temperature is significantly affected by the proximity of the molten iron outer core. We ask under what conditions this heated and therefore positively buoyant boundary layer will become unstable and rise to become the base of a plume. And if it does become unstable, which of all possible wavelengths will grow the most rapidly. The initial thickness of the buoyant layer is assumed to be perturbed with an initial thickness  $h$  and half-wavelength  $W$ . We will work two end-member cases, one in which the width of the perturbation is significantly greater than the thickness of the mantle,  $D$ , the other in which it is much shorter than the thickness of the mantle.

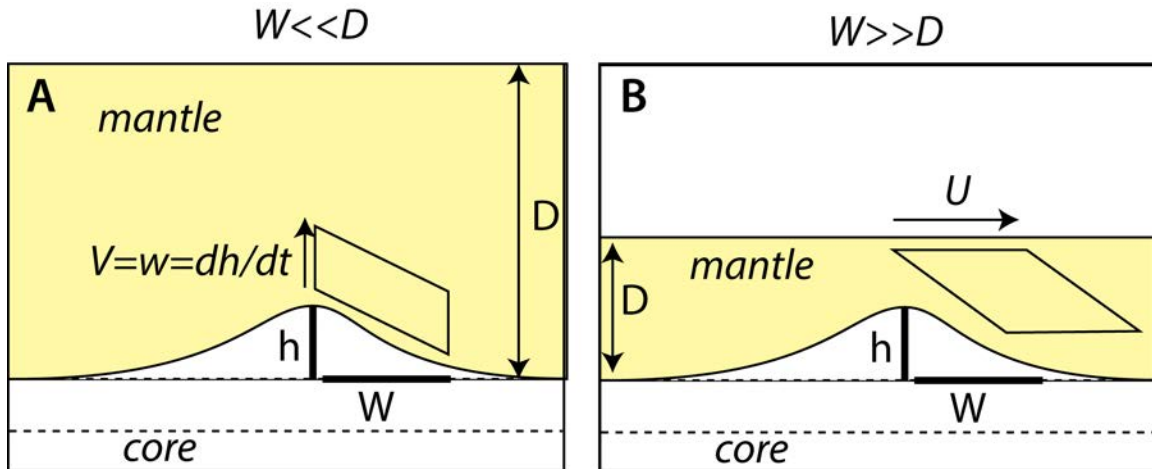


**Figure 1.** Plume instability sketch. A) Short wavelength case. B) Long wavelength case.

**Short wavelength case:  $W \ll D$ .**

Our goal is to craft an equation for the rate of change of  $h$ ,  $dh/dt$ . We assess both the buoyant forces promoting growth of the perturbation, as well as the viscous resisting forces. We then set these equal and evaluate the expected evolution of the thickness.

**Buoyant driving force:** The buoyant force is the product of the volume per unit length of the perturbation with the change in density associated with the heating – much as in a settling problem:

$$B = Wh\Delta\rho g \tag{14.1}$$

We evaluate this per unit length because we assume that the problem is axially symmetric. The buoyant weight increases linearly with the width of the perturbation.

**Viscous resisting force:** Here the trick is to assess the product of the shear stress acting on the edge of the (half) perturbation, with the length of that surface,  $W$ :

$$R = \tau W \tag{14.2}$$

The question is now how to assess this resisting shear stress. We appeal to Newton’s viscous rheology in which a shear stress is linearly related to the shear strain rate through the viscosity. But how do we calculate the relevant shear strain rate? Here is where our end-members come in. For the case at hand, with  $W \ll D$ , the main sense of motion of the overlying fluid will be  $dw/dx$ , where  $w$  is as always the vertical speed of the fluid, and  $x$  is the horizontal distance, as depicted in Figure 1A. We may approximate this relevant shear strain rate as  $V/W$  where  $V$  is the vertical velocity of the top of the perturbation. Hence

$$R = \mu \left( \frac{V}{W} \right) W = \mu V = \mu \frac{dh}{dt} \quad (14.3)$$

In the last equality we recognize that the speed of the fluid atop the perturbation is equivalent to the rate of growth of the perturbation, in other words  $V=dh/dt$ . We may now equate the resisting and driving forces to find that

$$\frac{dh}{dt} = \frac{\Delta\rho g W}{\mu} h = \frac{h}{t_s} \quad (14.4)$$

To construct the final equality we have recognized that the collection of constants beside  $h$  in the first equation must have units of 1/time. We have therefore defined a time scale relevant to the short wavelength ( $W \ll D$ ) case as

$$t_s = \frac{\mu}{\Delta\rho g W} \quad (14.5)$$

But before we go on, let's visualize what the history of the perturbation would be if equation 4 in fact captures the rate of growth. The solution to this ordinary differential equation is

$$h = h_0 e^{t/t_s} \quad (14.6)$$

Two features of this solution are easily noted. First, since  $t_s$  is always positive, all perturbations grow. The argument of the exponential is always positive. And the shorter  $t_s$  is, the faster it will grow. (Recall that at time  $t = t_s$   $h = e * h_0$ .) Second, inspection of equation 5 suggests that the dependence of the timescale for exponential growth on the wavelength of the perturbation is hyperbolic. In other words,  $t_s \sim 1/W$ , as shown in Figure 2. We can anticipate this behavior by inspecting the driving and resisting forces. The longer the perturbation, the greater the driving stress. But the resisting stress in this case (equation 3) is independent of the width of the perturbation. Hence the wider it is the greater the growth rate (and the smaller the characteristic timescale for growth).

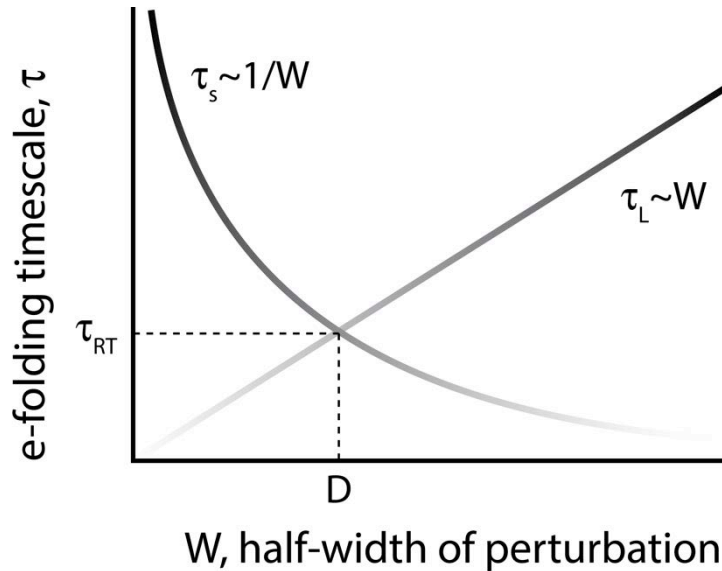


**Figure 2.** Timescales of growth of perturbations. Two end-member cases shown decay in boldness in realms where the assumptions behind the calculation break down.

But we have just said that the wider the perturbation the faster it should grow. At some point our assumption that  $W$  is short, i.e.  $W \ll D$ , will be violated. So we must perform the other end-member case.

**Long wavelength case:  $W \gg D$**

Now consider our other end-member (Figure 1B). Again, we assess the buoyant driving and viscous resisting forces.

**Buoyant driving force:** This is simple. The buoyant forces are again given by equation 1. The buoyant driving force linearly increases with wavelength of the perturbation.

**Viscous resisting force:** Here the fluid is being distorted in a different sense. The main shear in the flow will be  $du/dz$ , where as always  $u$  is the velocity in the horizontal dimension, and  $z$  is the vertical coordinate. This may be written

$$R = \tau W = \mu \frac{du}{dz} W = \mu \frac{U}{D} W \tag{14.7}$$

This is all well and good, but we require an expression that contains the vertical speed, not the horizontal speed. Here we appeal to continuity. In an incompressible medium the product of the vertical velocity with the width of the perturbation must equal the product of the horizontal velocity with the thickness of the layer (here the whole mantle). In other words:

$$WV = UD \tag{14.8}$$

Rearranging this for  $U$ , and substituting in equation 6 yields our final expression for the resistance:

$$R = \mu \frac{WV}{D^2} W = \mu \frac{W^2}{D^2} V = \mu \frac{W^2}{D^2} \frac{dh}{dt} \quad (14.9)$$

Again equating the buoyant and resisting forces results in our evolution equation for the perturbation:

$$\frac{dh}{dt} = \frac{\Delta\rho g D^2}{\mu W} h = \frac{h}{t_L} \quad (14.10)$$

As in the short wavelength case, we have recognized that the collections of constants in front of the  $h$  must have units of 1/time, and have defined the characteristic time scale for the long wavelength case to be

$$t_L = \frac{\mu W}{\Delta\rho g D^2} \quad (14.11)$$

This has a very different behavior than the short wavelength end-member. The timescale *increases* linearly with the width of the perturbation, meaning its growth rate declines with increasing width. That means that the predicted fastest growing perturbations will be at the shortest wavelengths...but that is exactly where the assumption of a long wavelength breaks down! I have plotted both of these timescales in Figure 2 to illustrate the problem. We can understand why this behavior occurs for the long end-member case by inspection of the equations for driving and resisting forces. While the driving force increases linearly with width (equation 1), the resisting force increases as the square of the width – so, much more rapidly than the driving force. Therefore the greater the width the more the resisting force wins.

It is clear that there is indeed a shortest timescale, hence a fastest growingest case, where the two curves cross (see Hanna and Barbera, 1959). Let us solve for where this occurs by setting our expressions for the short and the long timescales equal. This yields the very simple result that this occurs when  $W=D$ . Plugging in  $D$  for  $W$  in either of the expressions therefore results in an expression for our shortest timescale, corresponding to the fastest growing perturbation:

$$t_{RT} = \frac{\mu}{\Delta\rho g D} \quad (14.12)$$

This is dubbed the Rayleigh-Taylor timescale because this problem was solved by both Lord Rayleigh and G.I. Taylor. The phenomenon we have addressed is called the Rayleigh-Taylor instability. The fastest growing perturbation, that which should set the

spacing of plumes, is  $W=D$ . Since this is the half-width of the perturbation, the full spacing between plumes should be about 6000 km.

OK. That solves what wavelength we might expect, but what about the timescale? Is it a century, a million years, or a billion years? We may calculate the Rayleigh-Taylor timescale by evaluating its constants. One may estimate a mantle viscosity of  $10^{22}$  Pa-s,  $g = 10 \text{ m/s}^2$ , and thickness of the mantle  $D=3000 \text{ km} = 3 \times 10^6 \text{ m}$ . The change in density is that associated with a change in temperature. As always, we appeal to a coefficient of expansion,  $\alpha$ , to relate the two:

$$\Delta\rho = -\rho_m \alpha \Delta T \quad (14.13)$$

For  $\alpha = 10^{-5}/^\circ\text{C}$ , and  $\Delta T = 300^\circ\text{C}$ , the change in density is  $12 \text{ kg/m}^3$ . This results in a timescale of  $3 \times 10^{13} \text{ s}$ , or about one million years.

To quickly review, we have developed two end-member scenarios, one in which the width (half-width actually),  $W$ , of the perturbation was  $\gg$  the thickness of the mantle,  $D$ , and the other in which  $W \ll D$ . In each case we found that all perturbations grew; in other words we found that the solution to the resulting differential equation was an exponential with a *positive* constant, so that  $dh/dt = h_0 \exp(t/\tau)$ , where  $\tau$  was a characteristic time scale. This is the e-folding timescale, so that at  $t=\tau$  the amplitude of the perturbation is e times bigger than it was at  $t=0$ . The shorter is  $\tau$ , the faster the perturbation grows. So the trick is to find the fastest growing one, the thinking being that the fastest growing perturbation ought to win the battle to become the dominant wavelength (or plume spacing) in the system.

We found that the functional dependence of the calculated time scale  $t$  on the wavelength of the perturbation differed between the two cases. In the case of the short wavelength perturbations, for which  $W \ll D$ , that timescale grew linearly with  $W$ . And in the long wavelength case, the timescale was hyperbolic on  $W$ , in other words  $t(W) \sim 1/W$ . When we plotted these time scales against the wavelength, we found that there must be a fastest growing perturbation where the two timescales were equal, i.e. where the two solutions crossed. Solving for this time scale, we found that they crossed where  $W=D$ , meaning that the fastest growing (shortest  $t$ ) perturbation ought to be where the spacing between incipient plumes is roughly  $2W$ .

### **Part II. Will plumes die before they mature?**

But we have so far dodged a piece of the physics in this analysis. We have neglected to honor the fact that these perturbations, when driven by thermal-related density differences, could be defeated if the conductive heat loss from the incipient plume was more rapid than the growth of the plume. Here we formalize that notion by calculating the timescale involved in losing heat by conduction. The strategy is to calculate a second time scale, and to contrast the two timescales, one for growth of the plume, the other for cooling off the plume conductively. If the conduction timescale is shorter than the growth timescale, the plume should be defeated, and ought not to survive.

So, what is the conductive timescale? Recall that in all conduction problems, timescales go as the square of the relevant length scale. We could therefore assert that an approximate timescale would be

$$t_{\kappa} = \frac{D^2}{\kappa} \quad (14.14)$$

The shorter the wavelength of the perturbation, the more rapidly it should cool by conduction. We may now compare these two timescales by crafting the ratio of the two, which, because it is a time scale over a timescale, is dimensionless:

$$Ra = \frac{t_{\kappa}}{t_{RT}} = \frac{\Delta\rho g D^3}{\kappa\mu} = \frac{\alpha\rho_o\Delta T g D^3}{\kappa\mu} \quad (14.15)$$

This is yet another of those pesky dimensionless numbers that arise in fluid mechanics. This one is called the **Rayleigh number**,  $Ra$ , and it signifies the relative importance of advection over conduction in thermal-fluid problems. If the timescale to kill the perturbation is short relative to the timescale to grow it,  $Ra$  will be small, and the perturbation will die. And vice versa.

One has to turn to experiments to determine the critical  $Ra$  required for convection. Experiments show that when  $Ra > 600-1000$ , convection is assured.

What is  $Ra$  for the mantle? (calculate it) We find that it is about  $3 \times 10^5$ ...orders of magnitude greater than the  $\sim 10^3$  critical for convection. The implication is that the mantle should indeed be convecting, and should be well stirred. This augments the arguments we have made from the calculation of the plate speeds.

## References

- Davies, G., 1999, *Dynamic Earth: Plates, Plumes and Mantle Convection*, Cambridge: Cambridge University Press.
- Davies, G., 2011, *Mantle Convection for Geologists*, Cambridge: Cambridge University Press.
- Hanna, W. and Barbera, J., 1959, *Quick Draw McGraw* (The high-falutin'est, *Fastest shootin'est*, Cowboy you ever saw). Screen Gems.